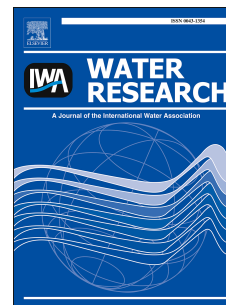


Accepted Manuscript

Comparison of endogenous metabolism during long-term anaerobic starvation of nitrite/nitrate cultivated denitrifying phosphorus removal sludges

Yayi Wang, Shuai Zhou, Hong Wang, Liu Ye, Jian Qin, Ximao Lin



PII: S0043-1354(14)00686-1

DOI: [10.1016/j.watres.2014.09.044](https://doi.org/10.1016/j.watres.2014.09.044)

Reference: WR 10907

To appear in: *Water Research*

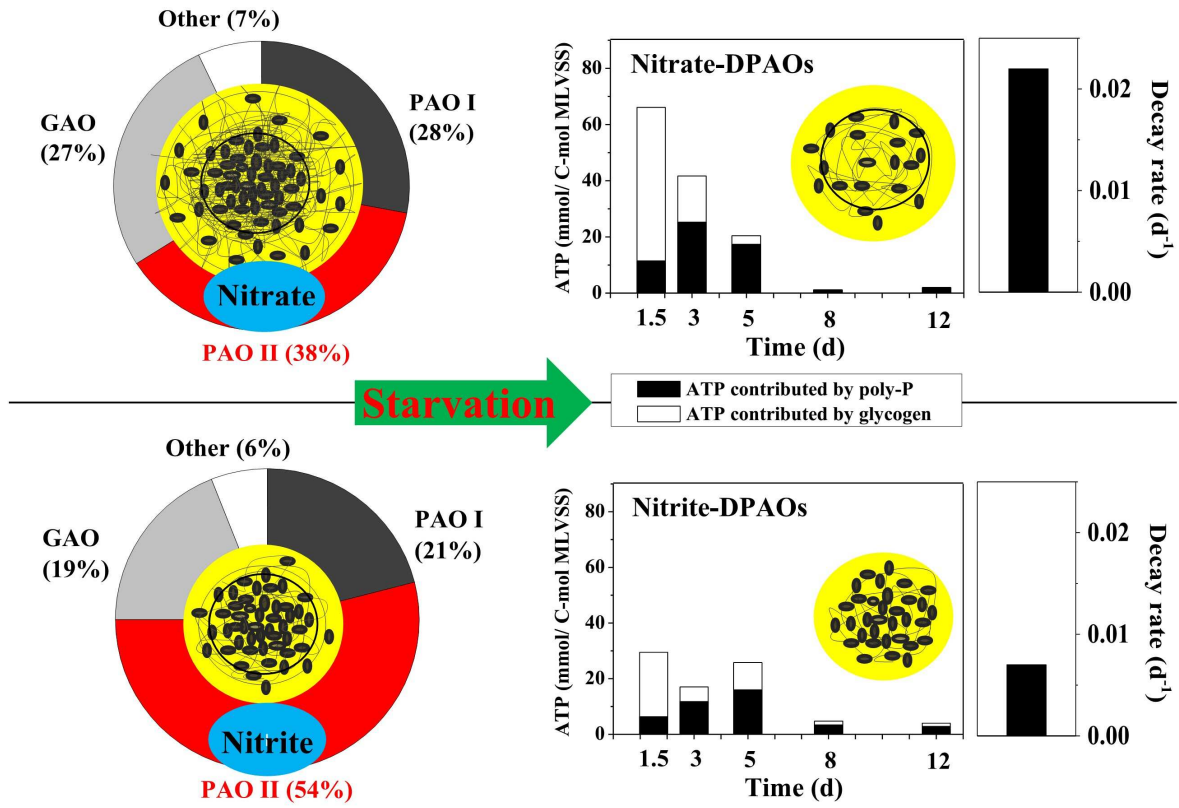
Received Date: 14 May 2014

Revised Date: 26 September 2014

Accepted Date: 28 September 2014

Please cite this article as: Wang, Y., Zhou, S., Wang, H., Ye, L., Qin, J., Lin, X., Comparison of endogenous metabolism during long-term anaerobic starvation of nitrite/nitrate cultivated denitrifying phosphorus removal sludges, *Water Research* (2014), doi: 10.1016/j.watres.2014.09.044.

This is a PDF file of an unedited manuscript that has been accepted for publication. As a service to our customers we are providing this early version of the manuscript. The manuscript will undergo copyediting, typesetting, and review of the resulting proof before it is published in its final form. Please note that during the production process errors may be discovered which could affect the content, and all legal disclaimers that apply to the journal pertain.



1 **Comparison of endogenous metabolism during long-term anaerobic starvation of**
2 **nitrite/nitrate cultivated denitrifying phosphorus removal sludges**

3
4 Yayi Wang^{1*}, Shuai Zhou¹, Hong Wang¹, Liu Ye², Jian Qin¹, Ximao Lin¹

5 *Corresponding author. Tel: +21 65984275; Fax: +21 65984275; E-mail:

6 yayi.wang@tongji.edu.cn

7
8 ¹State Key Laboratory of Pollution Control and Resources Reuse, College of
9 Environmental Science and Engineering, Tongji University, Siping Road, Shanghai
10 200092, P. R. China

11 ²School of Chemical Engineering, The University of Queensland, St Lucia, Brisbane
12 4072, Australia

13
14 **Abstract:** Denitrifying phosphorus removal (DPR) by denitrifying
15 phosphorus-accumulating organisms (DPAOs) is a promising approach for reducing
16 energy and carbon usage. However, influent fluctuations or interruptions frequently
17 expose the DPAOs biomass to starvation conditions, reducing biomass activity and
18 amount, and ultimately degrading the performance of DPR. Therefore, a better
19 understanding of the endogenous metabolism and recovery ability of DPAOs is
20 urgently required. In the present study, anaerobic starvation (12 days) and recovery
21 were investigated in nitrite- and nitrate-cultivated DPAOs at 20 ± 1 °C. The cell decay

22 rates in nitrite-DPAO sludges from the end of the anaerobic and aerobic phase were
23 0.008 day^{-1} and 0.007 day^{-1} , respectively, being 64% and 68% lower than those of
24 nitrate-DPAO sludges. Nitrite-DPAO sludges also recovered more rapidly than
25 nitrate-DPAO sludge after 12 days of starvation. The maintenance energy of
26 nitrite-DPAO sludges from the end of the anaerobic and aerobic phase were
27 approximately 31% and 34% lower, respectively, than those of nitrate-DPAO sludges.
28 Glycogen and polyphosphate (poly-P) sequentially served as the main maintenance
29 energy sources in both nitrite- and nitrate-DPAO sludges. However, the transformation
30 pathway of the intracellular polymers during starvation differed between the sludges.
31 Nitrate-DPAO sludge used extracellular polymeric substances (EPS) (mainly
32 polysaccharides) as an additional maintenance energy source during the first 3 days of
33 starvation. During this phase, EPS appeared to contribute to 19 – 27% of the ATP
34 production in nitrate-DPAOs, but considerably less to the cell maintenance of
35 nitrite-DPAOs. The high resistance of nitrite-DPAOs to starvation might be
36 attributable to frequent short-term starvation and exposure to toxic substances such as
37 nitrite/free nitrous acids in the parent nitrite-fed reactor. The strong resistance of
38 nitrite-DPAO sludge to anaerobic starvation may be exploited in P removal by
39 shortcut denitrification processes.

40

41 **Keywords:** Starvation; Denitrifying phosphorus-accumulating organisms;

42 Maintenance; Intracellular polymers; Extracellular polymeric substances; Decay

43 **1. Introduction**

44 Owing to large fluctuations in the flow and composition of wastewater, the
45 microorganisms responsible for biological wastewater treatment plants are frequently
46 exposed to long-term famine conditions (days and sometimes weeks) (Lu et al., 2007).
47 During sludge storage, by which large influent variations can be adjusted and flexible
48 plant operation can be achieved, microorganisms may experience starvation
49 (Morgenroth et al., 2000). Starvation significantly reduces the amount and activity of
50 active microorganisms, and risks degrading the capacity, efficiency and robustness of
51 wastewater treatment systems (Hao et al., 2010b; Wang et al., 2013b). Starvation is
52 crucially important in enhanced biological phosphorus removal (EBPR) processes,
53 since it alters the levels of intracellular storage compounds in the functional microbes
54 (i.e., polyphosphate-accumulating organisms, PAOs) (Vargas et al., 2013). Indeed,
55 excessive consumption of intracellular polymers (Yilmaz et al., 2007) or excessive
56 decay of both PAOs and intracellular polymers (Miyake and Morgenroth, 2005) has
57 been implicated in EBPR failure.

58 In the absence of external sustenance, starved microorganisms primarily undergo
59 the endogenous processes consisting of cell maintenance and cell decay (Lu et al.,
60 2007; Wang et al., 2012). The impacts of starvation on PAOs and endogenous
61 processes have been extensively investigated (Lopez et al., 2006; Yilmaz et al., 2007;
62 Lu et al., 2007; Hao et al., 2010a; Wang et al., 2012; Vargas, et al., 2013), and
63 effective strategies for maintaining the biomass activity have been accordingly

64 proposed. Lopez et al. (2006) examined the effects of long-term (weeks) anaerobic
65 and aerobic starvation on the composition and activity of PAOs. They concluded that,
66 under aerobic starvation conditions, PAOs are notably attenuated by endogenous
67 processes, whereas no significant PAOs decay occurs under anaerobic starvation. Lu
68 et al. (2007) proposed an intermittent aerobic–anaerobic strategy for the long-term
69 storage of EBPR sludge. In this strategy, the PAOs decay more slowly than in aerobic
70 storage, and glycogen and poly-P are used at a slower rate than in anaerobic and
71 anoxic storage. A similar recovery strategy was recommended by Yilmaz et al. (2007),
72 who found that alternating anoxic/anaerobic and aerobic operation effectively
73 maintains the biomass activity of activated sludge used for biological nitrogen (N) and
74 phosphorus (P) removal, thereby enabling quick activity recovery (i.e., full recovery
75 within 4 days).

76 Unlike PAOs in traditional EBPR processes, the impacts of starvation on
77 denitrifying polyphosphate-accumulating organisms (DPAOs) have been little
78 reported. Denitrifying phosphorus removal (DPR) by DPAOs is a viable and
79 sustainable technology, as N and P can be simultaneously removed with lower carbon
80 source requirements, aeration costs and cell yields (Murnleitner et al., 1997). In
81 particular, since DPAOs can use nitrite as an electron acceptor, DPR is naturally
82 amenable to shortcut nitrification. By replacing nitrate with nitrite, the oxygen cost
83 and carbon consumption of DPR can be reduced by approximately 25% and 40%,
84 respectively (Abeling et al., 1992). Therefore, DPR by nitrite could be used for

85 innovative biological nutrient removal (BNR) systems where energy and carbon
86 savings are a priority, for example, linking nitrite pathways (i.e., partial nitrification +
87 nitrite-based denitrification) to EBPR (Guisasola et al., 2009; Marcelino et al., 2011;
88 Zhou et al., 2011; Tayà et al., 2013). Moreover, as nitrite enriched PAOs need less
89 carbon source (i.e., intracellular PHA) for P-uptake, and eventually they might have
90 higher PHA accumulation which can be used to speed up their anoxic metabolism
91 after the endogenous period.

92 Recently, identifying the inhibitory effects of nitrite and the feasibility of
93 nitrite-based DPR has received increasing attention (Guisasola et al., 2009; Marcelino
94 et al., 2011; Zhou et al., 2011). However, DPAOs metabolism, especially their
95 endogenous metabolism, has not been properly elucidated. To our knowledge, the
96 endogenous characteristics of nitrite metabolism of DPAOs have not been assessed. A
97 better understanding of the mechanism of the impact of starvation on nitrite- and
98 nitrate-DPAOs, and endogenous metabolism of DPAOs may favor the development
99 of strategies for improvement of the robustness and performance of DPR processes,
100 the resuscitation of DPR systems after famine scenarios, and the storage of DPAOs
101 sludge.

102 Increasing evidence shows that extracellular polymeric substances (EPS) can
103 serve as carbon and energy sources for active biomass growth under starvation
104 conditions (Zhang and Bishop, 2003; Wang et al., 2005; Wang et al., 2007; Liu et al.,
105 2007; Flemming et al., 2010). Wang et al. (2005) found that most biodegradable EPS,

106 especially polysaccharides, are located in the core of aerobic granular sludge, and that
107 this fraction of EPS can be depleted after long-term starvation (20 days), as evidenced
108 by the void structure in the core of starved granules. Since most previous starvation
109 investigations of EBPR sludge did not involve EPS, the contribution of EPS to the
110 maintenance of metabolic activity of PAOs/DPAOs remains unclear.

111 The purpose of this study is to identify the differences between the endogenous
112 characteristics of nitrite- and nitrate-DPAO sludges during 12-day anaerobic
113 starvation, and to better understand the endogenous metabolism of nitrite-DPAOs. The
114 transformation of intracellular polymers and post-starvation activity recovery are also
115 compared between nitrite and nitrate-DPAO sludges. We highlight the different
116 transformation pathways of intracellular polymers in nitrite- and nitrate-DPAOs
117 biomass. We also attempt to clarify the role of EPS (especially polysaccharides) in
118 nitrite/nitrate-DPAOs under anaerobic starvation conditions.

119 **2. Materials and methods**

120 **2.1. Set up and long-term operation of parent reactors**

121 DPAOs sludge was enriched in two identical laboratory-scale sequencing batch
122 reactors ($SBR_{NO_3^-}$ and $SBR_{NO_2^-}$, using nitrate and nitrite as electron acceptors,
123 respectively) with a working volume of 7.5 L as outlined by Wang et al. (2011). Both
124 SBRs were independently operated in a cyclical anaerobic-anoxic-aerobic pattern
125 with a cycle time of 8 h (15-min filling period, a 120-min anaerobic period, a 210-min
126 anoxic period, a 30-min aerobic period, a 20-min settling period, a 15-min effluent

127 discharging period, and a 70-min idle period). During the filling period, each reactor
128 was fed with 5.5 L synthetic wastewater (*Section 2.2*). KNO_3 or KNO_2 solution was
129 carefully added to the reactors during the anoxic phase to prevent nitrate or nitrite
130 accumulation. Specifically, 34 mL KNO_3 solution was added to A-SBR_{NO₃⁻}, giving an
131 initial NO_3^- -N concentration of 34 mg/L; 11 mL KNO_2 solution was added into
132 A-SBR_{NO₂⁻} in three pulses (70 min of intervals), giving an initial NO_2^- -N
133 concentration of 11 mg/L per pulse. Effluent was withdrawn from the port at 30 cm
134 above the bottom, leaving 2.0 L of mixed liquor in the reactor.

135 The temperature was maintained at 20 ± 1 °C, and the rotation speed was
136 controlled at 150 ± 10 rpm during the reaction phases. Nitrogen gas was introduced
137 through the headspace for 5 min to ensure anaerobic condition at the beginning of the
138 anaerobic phase of each cycle. In the post-aerobic phase, the dissolved oxygen (DO)
139 concentration was controlled at 2 – 4 mg/L. The hydraulic retention time (HRT) was
140 10.9 h. To maintain the concentration of the mixed liquid suspended solids (MLSS) at
141 4000 ± 200 mg/L, 125 mL of mixed liquor was periodically discarded at the end of
142 each aerobic period. The solid retention time (SRT) under these conditions was
143 approximately 20 days.

144 **2.2. Synthetic wastewater**

145 The synthetic wastewater used in this study contained (per L): 257.1 mg
146 $\text{CH}_3\text{CH}_2\text{COONa}$ (300 mg chemical oxygen demand (COD)); 32.9 mg KH_2PO_4 (7.5
147 mg P); 55.3 mg $\text{K}_2\text{HPO}_4 \cdot 3\text{H}_2\text{O}$ (7.5 mg P); 38.2 mg NH_4Cl ; 85.0 mg $\text{MgSO}_4 \cdot 7\text{H}_2\text{O}$;

148 10.0 mg CaCl₂. Therefore, the influent volatile fatty acid (VFA, i.e., propionate) to P
149 ratio was 6.4 mg C/mg P. PAOs were preferentially selected by adding propionate as
150 the sole carbon source (Oehmen et al., 2005). Trace salt solution (0.3 mL/L) and
151 allylthiourea (4 mg/L) were added as described by Wang et al. (2011). The pH of the
152 synthetic wastewater was maintained at 7.5 ± 0.1 by adding NaHCO₃.

153 **2.3. Starvation batch experiments**

154 Once the SBRs had reached steady-state operation, batch experiments were conducted
155 in four identical sealed reactors, each with a working volume of 3.8 L and an
156 overhead space of 0.2 L. The long-term nitrate or nitrite cultivated sludge in SBR_{NO₃-}
157 and SBR_{NO₂-} was divided into two equal portions at the end of the decanting phase,
158 and was then transferred to one of the four batch reactors. For each starvation test, 2.8
159 L synthetic wastewater was rapidly added to each reactor, maintaining the MLSS
160 level at 4000 ± 200 mg/L. One of the two reactors incubated with nitrate-DPAOs
161 sludge was operated with a 2-h anaerobic reaction (A-R_{NO₃-}), the other was operated
162 with a 2-h anaerobic reaction, a 3.5-h anoxic reaction and a 0.5-h aerobic reaction
163 (O-R_{NO₃-}). The corresponding nitrite-DPAOs sludges (operated under the same
164 conditions) from the end of the anaerobic and aerobic phases are called A-R_{NO₂-} and
165 O-R_{NO₂-}, respectively. After one operation cycle, each reactor was sparged with
166 nitrogen gas for 10 min to maintain anaerobic conditions, and was left idle for the
167 next 12 days. During the starvation experiments, each reactor was sparged with
168 nitrogen gas for 10 min per day to remove any H₂S accumulated by the activity of

169 sulfate-reducing bacteria (Morgenroth et al., 2000; Yilmaz et al., 2007). All tests were
170 carried out at 20 ± 1 °C, and the pH was manually controlled at 7.5 ± 0.1 by adding
171 0.3 M HCl or 0.3 M NaOH.

172 Liquid- and solid-phase samples were taken from each reactor on days 0, 1.5, 3, 5,
173 8, and 12. The mixed liquor was filtered through a Millipore filter unit (pore size =
174 0.45 μm), and the liquid portion was retained for analysis of VFA, NH_4^+ -N, PO_4^{3-} -P,
175 NO_3^- -N and NO_2^- -N. The solid portion (biomass) was centrifuged, freeze-dried and
176 retained for analysis of intracellular polymers, including poly- β -hydroxybutyrate
177 (PHB), poly- β -hydroxyvalerate (PHV), poly-3-hydroxy-2-methylvalerate (PH2MV),
178 and glycogen. Samples were also taken for MLSS, mixed liquor volatile suspended
179 solids (MLVSS) and EPS measurements.

180 **2.4. Recovery batch experiments**

181 After 12 days of starvation, the biomass activities of the starved nitrite/nitrate DPAO
182 sludges were assessed in batch tests. The sludges in the four batch reactors were
183 washed three times with 2.8 L propionate-free synthetic wastewater. At the beginning
184 of the recovery test, 2.8 L of propionate-free synthetic wastewater was rapidly added
185 to the reactors containing activated sludge from the end of the anaerobic phase
186 (denoted $\text{AS}_{\text{ANA.end}}$) (A- $\text{R}_{\text{NO}_3^-}$ - and A- $\text{R}_{\text{NO}_2^-}$). The anoxic reaction (3.5 h) was started by
187 adding $\text{KNO}_3/\text{KNO}_2$ as described in *Section 2.1*, followed by a 0.5-h aerobic reaction.
188 The reactors containing activated sludge from the end of the aerobic phase (denoted
189 $\text{AS}_{\text{AER.end}}$) (O- $\text{R}_{\text{NO}_3^-}$ - and O- $\text{R}_{\text{NO}_2^-}$) were rapidly supplemented with 2.8 L of synthetic

190 wastewater at the beginning of the recovery test, and then were directly operated
191 through the typical cycle for SBR_{NO3-} and SBR_{NO2-}, respectively. Two recovery cycles
192 were applied to each of these four reactors.

193 **2.5. Analytical methods**

194 Liquid- and solid-phase analyses of NH₄⁺-N, NO₃⁻-N, NO₂⁻-N, PO₄³⁻-P, MLSS and
195 MLVSS were performed by the standard method (APHA, 1998). DO and pH were
196 measured online using oxygen and pH meters (oxi 3310 and pH 3310, WTW
197 Company, Germany), respectively. Glycogen, poly-β-hydroxyalkanoates (PHA), VFA,
198 and EPS were determined by the procedure detailed in the Supplementary Information
199 (SI) (Text S1). PHA content in the sludge sample was defined as the sum of the
200 measured PHB, PHV and PH2MV. EPS was extracted by the formaldehyde-NaOH
201 method, and was calculated as the sum of polysaccharides, proteins and humic
202 substances.

203 The relative PAOs and glycogen-accumulating organisms (GAOs) abundances in
204 both parent SBRs were estimated by 16S rRNA fluorescence in situ hybridization
205 (FISH), as described in Wang et al. (2013b). *Candidatus Accumulibacter phosphatis*
206 (hereafter referred to as *Accumulibacter*), *Candidatus Competibacter phosphatis*
207 (hereafter referred to as *Competibacter*), *Defluvicoccus*-related TFO, and
208 *Defluvicoccus*-related DF were targeted by appropriate oligonucleotide probes (Text
209 S2 and Table S1).

210 2.6. Determination of cell decay rate

211 The decay rate of DPAOs was estimated from the measured NH_4^+ -N release rate
212 based on the activated biomass composition ($\text{CH}_{2.09}\text{O}_{0.54}\text{N}_{0.20}\text{P}_{0.015}$) (Smolders et al.,
213 1994), i.e., primarily based on the reduction in the amount of bacteria. The MLVSS is
214 assumed as the sum of PHA, glycogen, and active biomass (Smolders et al., 1995).
215 Thus, the active biomass is estimated by subtracting the PHA and glycogen content
216 from the MLVSS. Accordingly, the decay rate is calculated based on Eq. (1) (Lesouef
217 et al., 1992):

$$218 \quad b = -\ln (X_t/X_0)/t_d \quad (1)$$

219 where b is the decay death rate of the PAOs, X_0 and X_t denote the active biomass
220 concentration (without glycogen and PHA) before and after starvation respectively,
221 and t_d is the duration of the starvation period.

222 3. Results

223 3.1. Performance of SBR_{NO_2} - and SBR_{NO_3} - and relevant microbial populations

224 The SBR_{NO_2} - and SBR_{NO_3} - steadily operated for 210 days. Typical cycle tests were
225 conducted during steady-state operation (Figure S1) and the DPAOs activities were
226 estimated from the biochemical reaction rates. The maximum rates of P release and
227 uptake, denitrification, and intracellular polymer transformations were higher for
228 nitrite DPAOs than those for nitrate-DPAOs (Table 1), indicating that DPAOs
229 activities are greater in the nitrite-fed than in the nitrate fed reactors.

230 FISH results show that *Accumulibacter*, bound to the PAOMIX probe, were the

231 dominant organisms in both reactors, comprising $66 \pm 1.5\%$ and $75 \pm 1.1\%$ of total
232 biomass in SBR_{NO3-} and SBR_{NO2-}, respectively (Table 1). The ratio of PAOII (unable
233 to use nitrate as an electron acceptor) to total PAOs was 57.6% and 72% in SBR_{NO3-}
234 and SBR_{NO2-}, respectively. *Defluvicoccus*-related GAOs were approximately $27 \pm 0.9\%$
235 and $19 \pm 0.6\%$ in SBR_{NO3-} and SBR_{NO2-}, respectively, while *Competibacter*-related
236 GAOs were nearly undetectable ($< 1\%$) in both SBRs (Table 1).

237 3.2. Anaerobic starvation in nitrite/nitrate DPAOs biomass

238 3.2.1 Release of $\text{NH}_4^+\text{-N}$ and $\text{PO}_4^{3-}\text{-P}$, and reduction of MLSS and MLVSS

239 Since the $\text{NH}_4^+\text{-N}$ profile reflects the biomass growth condition, it is a useful tool for
240 determining the cell decay of DPAOs (Zeng et al., 2003b; Lu et al., 2007). In all
241 reactors, the $\text{NH}_4^+\text{-N}$ concentrations increased gradually during the first 3 days of
242 starvation and rapidly thereafter (Figure 1a), indicating the increasing extent of cell
243 decay. Within 12 days of starvation, cell decay (including cell lysis and the respiration
244 of intracellular materials) released 41.8 mg, 39.5 mg, 18.7 mg and 15.8 mg of
245 $\text{NH}_4^+\text{-N/L}$ into the liquid phase of A-R_{NO3-}, O-R_{NO3-}, A-R_{NO2-} and O-R_{NO2-},
246 respectively (Figure 1a and Table 2). The ammonia release rates were clearly much
247 higher in nitrate-DPAO sludges than those in nitrite-DPAO sludges (Table 2), whereas
248 no appreciable difference was observed in the $\text{NH}_4^+\text{-N}$ release rates between
249 $\text{AS}_{\text{ANA.end}}$ and $\text{AS}_{\text{AER.end}}$ (Figure 1a).

250 The starvation period in all reactors was also marked by P release, as
251 intracellular poly-P was degraded to obtain energy for maintenance processes.

252 Specifically, the P release rate was elevated during day 1 – 5 in all reactors; thereafter,
253 the P concentration in the bulk remained constant (Figure 1b). Correspondingly, the
254 MLSS concentrations gradually decreased during the first 5 days (Figure 2a). Notably,
255 the MLSS concentration decreased less in nitrite-DPAO sludges (A-R_{NO2-} and O-R_{NO2-})
256 than those in nitrate-DPAO sludges (A-R_{NO3-} and O-R_{NO3-}) (Figure 2a). These findings
257 are related to the lower P release rate in A-R_{NO2-} and O-R_{NO2-} (Table 3). Among these
258 reactors, the MLSS and MLVSS concentrations were most heavily reduced in O-R_{NO3-},
259 largely because the storage products (especially glycogen and poly-P) were most
260 depleted in this reactor, accounting for approximately 51% and 33% of the decrease
261 of MLVSS and MLSS, respectively, in O-R_{NO3-} (Table 3). Similarly, Lopez et al.
262 (2006) reported that maintenance processes utilizing organic (PHA and glycogen) and
263 inorganic (poly-P) storage products accounted for about 23% and 29% of the aerobic
264 decrease of MLVSS and MLSS, respectively. The MLVSS, MLSS and MLVSS/MLSS
265 variations in AS_{ANA.end} were comparable to those in AS_{AER.end} from the same parent
266 SBR (Figure 2).

267 **3.2.2 Variations in glycogen and PHA contents**

268 In all four reactors, most of the glycogen was consumed within the first 5 days (Figure
269 3). The glycogen degradation was approximately 21% and 38% lower in the AS_{ANA.end}
270 and AS_{AER.end} sludges, respectively, when compared with those in their nitrate-DPAO
271 sludge counterparts (Figure 3 and Table 3). These findings indicate a relatively lower
272 energy requirement for glycogen hydrolysis in nitrite-DPAOs, and may also correlate

273 with the lower GAO percentage in nitrite-DPAO sludge ($19 \pm 0.6\%$) than in
274 nitrate-DPAO sludge ($27 \pm 0.9\%$) (Table 1). Moreover, the amounts of glycogen
275 degradation were much lower in $AS_{ANA.end}$ (A-R_{NO3-} and A-R_{NO2-}) than those in
276 $AS_{AER.end}$ (O-R_{NO3-} and O-R_{NO2-}). Since glycogen had been partially degraded by
277 anaerobic reactions to supply reducing equivalents before the starvation test, it is
278 likely that less glycogen was available for $AS_{ANA.end}$ as compared to that for $AS_{AER.end}$.
279 These findings agree with our previous observation (Wang et al., 2012) that glycogen
280 degradation rate is approximately 48% lower for $AS_{ANA.end}$ than for $AS_{AER.end}$ after 7
281 days of anaerobic starvation at 15 °C.

282 PHA was synthesized during the 12 starvation days in all four reactors. Most of
283 the PHA was synthesized during the first 5 days (Figure 3), corresponding to the high
284 glycogen degradation. The main PHA components of nitrite- and nitrate-DPAO
285 sludges fed with propionate as the sole carbon source were PH₂MV and PHV (Table
286 3). During the 12 days of starvation more PHA was synthesized by $AS_{ANA.end}$ in
287 A-R_{NO2-} (2.79 mmol-C/g-MLVSS) than that by $AS_{ANA.end}$ in A-R_{NO3-} (1.84
288 mmol-C/g-MLVSS) (Table 3), and the PHA synthesis rate in A-R_{NO2-} was almost
289 twice that in A-R_{NO3-}. Similar results were obtained for $AS_{AER.end}$, suggesting that
290 most of the degraded glycogen was converted to PHA in the nitrite-DPAO sludges.

291 **3.2.3 Variations in EPS amounts and compositions**

292 EPS production is essential for the survival of *Accumulibacter* in wastewater
293 treatment systems (Martín et al., 2006). As a candidate carbon and energy source,

294 EPS degradation allows the microorganisms to rapidly adapt to varying influent
295 composition, temperature (Martín et al., 2006) and substrate limitation (Zhang and
296 Bishop, 2003). However, the contribution of EPS to the anaerobic endogenous
297 metabolism of DPAOs has not been previously reported. We also report the first
298 description of EPS variations during anaerobic starvation of DPAO sludges.

299 Figure 4 presents the EPS profiles after 3 and 12 days of starvation. The initial
300 amounts of EPS in A-R_{NO2-} and O-R_{NO2-} sludges were approximately 17.0 and 11.5%
301 lower, respectively, than those in their A-R_{NO3-} and O-R_{NO3-} counterparts (Figure 4d).
302 This discrepancy is attributable to the different polysaccharides content in the EPS of
303 different sludges. In particular, polysaccharides synthesis may be prevented by the
304 presence of free nitrous acid (FNA) in nitrite-DPAOs (Wang et al., 2013a).
305 Specifically, the initial polysaccharides content of EPS was 60.8% and 71.3% higher
306 in A-R_{NO3-} and O-R_{NO3-} than those in A-R_{NO2-} and O-R_{NO2-}, respectively (Figure 4b).
307 Polysaccharides degradation in A-R_{NO3-} and O-R_{NO3-} was almost complete within 3
308 days of starvation (Figure 4b). Similarly, Wang et al. (2007) reported a sharp decrease
309 (approximately 50%) in the polysaccharides content of EPS in highly resistant aerobic
310 granules starved for 4 days. In A-R_{NO2-} and O-R_{NO2-}, polysaccharides degradation
311 throughout the first 3 days was only 3.7 ± 0.2 mg/g MLVSS and 1.2 ± 0.0 mg/g
312 MLVSS respectively, accounting for approximately 32% and 12% of the total
313 polysaccharides content, respectively (Figure 4b). At the end of the starvation on day
314 12, the polysaccharides contents remained low in all reactors.

315 The proteins changes in the four reactors greatly differed from the
316 polysaccharides changes (Figure 4a and b). The proteins content in all reactors
317 slightly increased during the first 3 days of starvation and had decreased to low levels
318 by day 12. It is speculated that, early in the starvation period, cell decay processes
319 released a portion of the intracellular proteins into the extracellular space, where it
320 was captured by EPS. Cellular decay is supported by the increased ammonia
321 concentration in all four reactors during the first 3 days of starvation (Figure 1a). At
322 the end of the starvation period, the proteins contents in all four reactors were heavily
323 reduced, suggesting that proteins may also be hydrolyzed or degraded by the
324 microorganisms as carbon and energy sources. The difference in EPS content
325 variations was negligible between $AS_{ANA.end}$ and $AS_{AER.end}$ from the same parent
326 (SBR_{NO_3-} or SBR_{NO_2-}).

327 **3.3. Recovery of nitrite- and nitrate-DPAOs activities after 12 days of starvation**

328 **3.3.1 Recovery of nitrite- and nitrate-DPAOs in $AS_{ANA.end}$**

329 Nitrite denitrification was completed during the first recovery cycle in both A- R_{NO_3-}
330 and A- R_{NO_2-} . The P uptake efficiency of nitrite-DPAOs was actually slightly increased
331 relative to the pre-starvation efficiency (Figure 5c and d; Figure S1 d). This increase
332 is attributed to the relatively lower “secondary” P release after nitrite depletion by
333 starved microorganism (1.6 mg PO_4^{3-} -P/L vs. 10.8 mg PO_4^{3-} -P/L in a typical
334 pre-starvation cycle). In contrast, the efficiencies of nitrate denitrification and anoxic
335 P uptake in starved nitrate-DPAOs sludge were decreased by 42.9% and 47.2%,

336 respectively, relative to their pre-starvation levels in a typical cycle (Figure 5a and b;
337 Figure S1c and d). The rapid recovery of nitrite-DPAOs activities indicates a higher
338 ability of these organisms to overcome starvation shock. The strong anoxic
339 denitrification and P uptake efficiency during starvation was also partially contributed
340 by PHA synthesis (Figure 3), which provides an electron donor and energy source for
341 the DPAOs. Moreover, the higher amounts of PHA synthesis by nitrite-DPAOs than
342 those by nitrate-DPAOs during the endogenous period (Table 3) may accelerate the
343 anoxic metabolism of nitrite-DPAOs during the recovery period, further benefitting
344 the stable operation of shortcut denitrification P removal systems.

345 In the second recovery batch test of $AS_{ANA.end}$, the concentration of the released P
346 reached 48.0 mg PO_4^{3-} -P/L and 47.3 mg PO_4^{3-} -P/L in $A-R_{NO_3-}$ and $A-R_{NO_2-}$
347 respectively, with a respective recovery percentage of 91.7% and 82.3%.

348 **3.3.2 Recovery of nitrite- and nitrate-DPAOs in $AS_{AER.end}$**

349 The VFA concentration in $O-R_{NO_3-}$ and $O-R_{NO_2-}$ ($AS_{AER.end}$) decreased from its initial
350 5.89 mmol C/L to 5.16 mmol C/L and 4.60 mmol C/L, respectively, at the end of the
351 anaerobic phases in the first recovery batch test (data not shown), representing a
352 decrease of 87.6% and 78.1%, respectively, compared with the amount of VFA
353 assimilated by their parents (SBR_{NO_3-} and SBR_{NO_2-}) in the anaerobic phase. Indeed,
354 during the anaerobic phase of both parent SBRs, the added VFA were completely
355 depleted within 30 minutes (Figure S1).

356 The total amount of released P also sharply declined in $O-R_{NO_3-}$ and $O-R_{NO_2-}$, by

357 86.9% and 79.4% respectively, relative to their corresponding values in the typical
358 parent SBRs (Table 4). This result may be attributed to rapid degradation of poly-P
359 during starvation, leaving minimal quantities of poly-P in DPAOs cells starved for 12
360 days. During the subsequent anoxic phases, the amount of P uptake in O-R_{NO₃⁻} and
361 O-R_{NO₂⁻} was only 4.1 and 5.7 mg PO₄³⁻-P/L respectively, indicating a severe
362 deterioration of P removal ability (Table 4). Nevertheless, the effluent P concentration
363 in O-R_{NO₂⁻} remained at 1.3 mg PO₄³⁻-P/L, suggesting that activity was recovered more
364 rapidly in nitrite-DPAOs sludge than in nitrate-DPAOs sludge (Figure 5b and d). In
365 contrast to the largely diminished P removal, the denitrification efficiencies during the
366 anoxic phase were similar to those observed during typical cycles of the parent SBRs.
367 This result is likely due to the presence of ordinary heterotrophs (OHOs) and
368 denitrifying glycogen-accumulating microorganisms (DGAOs), which might use the
369 residual VFA of the anaerobic phase for anoxic denitrification.

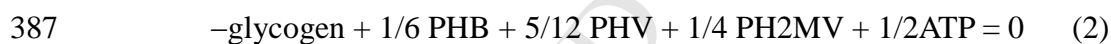
370 **4. Discussion**

371 The endogenous processes of PAOs can be differentiated into two aspects: (i)
372 maintenance processes linked to utilization of intracellular polymers (mainly poly-P
373 and glycogen) and EPS, which maintain cellular integrity and activity; and (ii) decay
374 processes, which reduce the amount and/or activity of the active biomass (Lopez et al.,
375 2006; Hao et al., 2010b).

376 **4.1. Cell maintenance in the nitrite/nitrate-DPAOs sludge**

377 *4.1.1 Energy and reducing equivalent sources from intracellular polymers*

378 While poly-P is consensually regarded as a maintenance source during anaerobic
379 starvation, glycogen is an important energy pool as well as an equivalent reducing
380 source for the maintenance of PAOs (Lopez et al., 2006; Lu et al., 2007; Wang et al.,
381 2012; Vargas et al., 2013). Under anaerobic conditions, glycogen is usually processed
382 for maintenance through a combination of glycolysis and the PHA production
383 pathway (Lopez et al., 2006; Lu et al., 2007). The main reactions involved in
384 glycogen degradation and PHA formation in nitrite- and nitrate-DPAOs were
385 described in details in previous studies (Filipe et al. 2001; Zeng et al. 2003a). The
386 overall reaction (in terms of the molar relationships) is given by Eq. (2):



388 PHA synthesis in the present starvation test is summarized in Table 3. The ratios
389 among PHB, PHV and PH₂MV in the nitrate-DPAOs sludge reactors are
390 well-predicted by Eq. (2). However, the proposed stoichiometry of anaerobic
391 maintenance does not adequately describe the composition of the PHA synthesized by
392 starved nitrite-DPAO sludges. The higher PH₂MV content suggests that the
393 investigated nitrite-DPAO sludges adopt different survival metabolic pathways in
394 their endogenous processes. This may correlate with a larger fraction of
395 propionyl-CoA (precursor of PH₂MV) produced from acetyl-CoA through the
396 methylmalonyl pathway, as reported by Yagci et al. (2003). Similarly, Oehmen et al.

397 (2006) analyzed the PHA composition in anaerobic test batch culture without
398 propionate addition, and obtained 12% PHB, 41% PHV and 47% PH2MV. They
399 attributed this result to enrichment of *Alphaproteobacteria* GAOs. The PHA synthesis
400 mechanism in nitrite-DPAOs during starvation is detailed in the SI (Text S3).

401 **4.1.2 Maintenance substrate and energy sources from EPS**

402 EPS is an important potential energy source that enables DPAOs to manage starvation
403 shock. In all reactors, EPS were almost completely depleted after 12 days of
404 starvation, and minimal non-biodegradable EPS remained in the sludge (Figure 4).
405 Especially, the easily biodegradable components of EPS (i.e., polysaccharides) were
406 rapidly utilized for maintenance during the initial starvation period, followed by
407 utilization of proteins (Figure 4a and b). Indeed, various extracellular enzymes have
408 been detected in activated sludge and biofilms, many of which can potentially degrade
409 EPS components to low-molecular-mass compounds that can then be utilized by
410 microorganisms as carbon and energy sources during starvation periods (Flemming et
411 al., 2010; Zhang and Bishop, 2003; Liu et al., 2007). The main degraders of EPS
412 polysaccharides are hydrolases and lyases (Laue et al., 2006), such as
413 N-acetyl- β -hexosaminidase (Kaplan et al., 2004). Metagenomic analysis of two EBPR
414 sludge communities has revealed the genes encoding enzymes for carbohydrate
415 polymer hydrolysis and subsequent monomer degradation pathways in the dominant
416 flanking species, namely, *Flexibacter*-like, *Xylella*-like and *Thiothrix*-like populations
417 (Martín et al., 2006). Martín et al. (2006) also reported that one of the EPS gene

418 cassettes in *Accumulibacter* encodes UDP-glucose dehydrogenase, which catalyzes
419 the precursor of the glucuronic acid component of EPS. Therefore, the dominant
420 flanking *Xylella*-like population may be able to degrade the glucuronic acid in
421 *Accumulibacter* EPS as a carbon and energy source. Additionally, EPS extracted from
422 biofilms were also found to be effectively degraded by their own producing
423 microorganism (Zhang and Bishop, 2003).

424 After 3 days of starvation, at least 90% less polysaccharides were degraded by
425 nitrite-DPAO sludges than by nitrate-DPAO sludges (Figure 4b). This result may be
426 ascribed to the relatively low initial polysaccharides content in the SBR_{NO2-} sludge. It
427 should also be mentioned that because the degradation pathway of proteins is more
428 complicated than that of polysaccharides, it is not certain that the decreased proteins
429 (in EPS) contents had been used as substrate to produce energy by cells or only had
430 been hydrolyzed or broken down into its component, i.e., amino acids. Since amino
431 acids in the bulk were not analyzed during the starvation period, the exact amount of
432 EPS proteins being degraded as substrate cannot be accurately determined, and
433 requires further study.

434 ***4.1.3 Energy production from intracellular polymers and EPS***

435 Maintenance energy is critical for the survival of nutrient-limited bacteria. PAOs
436 generally use poly-P and glycogen as maintenance energy sources under anaerobic
437 starvation conditions (Lopez et al., 2006; Lu et al., 2007). However, the main source
438 between them has yet to be clarified. Lu et al. (2007) found that, early in the

439 starvation period, PAOs prefer glycogen to poly-P as an energy source. In contrast,
440 Lopez et al. (2006) found that PAOs sequentially consume poly-P and glycogen,
441 which is supported by lack of any P released during the first day of starvation. No
442 glycogen degradation was observed during an 8-hour anaerobic starvation batch test
443 (Oehmen et al., 2005), supporting the assumption that PAOs use their stored poly-P as
444 the sole source of maintenance energy. Therefore, in the present study, we examined
445 the energy produced by both glycogen and poly-P. Moreover, the polysaccharides in
446 EPS were considered as a potential additional maintenance energy source when
447 calculating the maintenance ATP (Text S4).

448 As shown in Figure 6, glycogen and poly-P were simultaneously utilized during
449 the first 3 days of starvation, similar to our previous observations (Wang et al., 2012).
450 Notably, the polysaccharides in EPS also contributed a sizeable fraction of the
451 maintenance energy, especially in nitrate-DPAO sludge (Figure 6a and b). Hydrolysis
452 of 1 mol poly-P presumably yields 1 mol ATP, while degradation of 1 mol-C glycogen
453 and 1 mol-C polysaccharides should each generate 0.5 mol ATP (Smolders et al.,
454 1994). Maintenance energy production by DPAOs under anaerobic conditions was
455 calculated from the amounts of glycogen consumed and P released (Table 3 and
456 Figure 4).

457 In all reactors, most of the ATP was produced during the first 5 days of starvation.
458 Glycogen was the primary maintenance energy source throughout the first 1.5 days,
459 contributing more than approximately 70% to the total energy production in all four

460 reactors (Figure 6a-d). During day 1.5 – 3, poly-P was increasingly used as an
461 alternative maintenance energy source, and its use dominated (contributed over 50%
462 of the total ATP production) on day 5 in all four reactors (Figure 6a-d). Similar
463 observation was also reported by Lu et al. (2007), who found that glycogen
464 degradation provided the majority of the energy on day 1, after which there was a
465 transition of the primary energy source from glycogen to poly-P. Whereas, Lopez et al.
466 (2006) observed a sequential utilization of poly-P and glycogen by PAOs for
467 maintenance energy production under anaerobic conditions. The reasons for this
468 discrepancy have not been presented. Moreover, as these two studies did not present
469 the data of the GAOs percentage, it is not easy to explain this discrepancy from the
470 microbial point of view (e. g., PAOs vs. GAOs). In the present study, we doubt that
471 this result might arise from the relatively high proportion of GAOs in both SBR_{NO3-}
472 ($27 \pm 0.9\%$ of the total biomass) and SBR_{NO2-} ($19 \pm 0.6\%$ of the total biomass) (Table
473 1). The major energy source of GAOs is glycogen, while poly-P hydrolysis supplies
474 energy for the dominant PAOs. In the nitrate-DPAOs sludges, polysaccharides
475 provided additional maintenance energy during the first 3 days of starvation, with
476 values of 16.2 and 20.3 ATP mmol/C-mol biomass for $AS_{ANA.end}$ and $AS_{AER.end}$,
477 accounting for 27% and 19% of the total energy production, respectively (Figure 6a
478 and b). After day 5, a marked decline in energy production was observed (Figure
479 6a-d). Such relatively low energy production may not meet the minimal energy
480 demands of DPAOs. The resulting cell lysis is evidenced in a sharp increase in

481 NH_4^+ -N concentration (Figure 1).

482 During the 12-day starvation, energy production of nitrite-DPAO sludges in
483 $AS_{ANA.end}$ and $AS_{AER.end}$ were estimated to be 31% and 34% lower, respectively, than
484 those of nitrate-DPAO sludges (Figure 6a-d). The relatively low requirement for
485 maintenance energy of nitrite-DPAOs is further supported by the constant amounts of
486 EPS polysaccharides within the first 3 days (Figure 4). This result may reflect a robust
487 starvation survival response in nitrite-DPAOs. Following each nitrite addition, the
488 parent SBR_{NO_2-} was exposed to episodes of famine (no nitrite was available during the
489 first 30 – 70 min of the anoxic period; see Figure S1b). Consequently, nitrite-DPAOs
490 relied on their internal poly-P and/or glycogen reserves for maintenance energy, as
491 evidenced by the irregular P release and glycogen consumption during the anoxic
492 phases of typical cycles (Figure S1d and f). Because of the frequent starvation
493 episodes, and the high number of nitrite/FNA shocks in the parent SBR_{NO_2-} , the
494 nitrite-DPAOs were primed to adjust their endogenous mechanisms by slowing down
495 their self-oxidation rate and lowering their maintenance energy, i.e., consuming less
496 glycogen and poly-P, to survive under the imposed starvation conditions. Thus,
497 acclimation of nitrite-DPAOs to the starved conditions may allow them higher
498 adaptability to starvation shock than their nitrate-DPAO counterparts. In addition,
499 $AS_{AER.end}$ required more energy than $AS_{ANA.end}$ (Figure 6a-d), primarily owing to the
500 lower energy available from glycogen and poly-P in $AS_{AER.end}$.

501 **4.2 Decay process of the nitrite/nitrate-DPAO sludges**

502 Cell decay refers to any process that reduces the weight (negative growth) and the
503 specific activity of biomass. The cell decay rates in A-R_{NO3-}, O-R_{NO3-}, A-R_{NO2-} and
504 O-R_{NO2-} were estimated to be 0.022, 0.022, 0.008 and 0.007 day⁻¹, respectively (Table
505 2). The cell decay rates were much lower in nitrite-DPAO sludges than in
506 nitrate-DPAO sludges, and were comparable to the value reported by Lu et al. (2007)
507 (0.006 day⁻¹) for PAOs under anaerobic starvation conditions.

508 As mentioned in *Section 4.1.3*, frequent starvation episodes in the parent
509 nitrite-SBR might evoke stringent starvation responses in the nitrite-DPAOs sludge.
510 In other words, nitrite-DPAOs possess a better survival strategy via a relatively low
511 maintenance energy requirement to ensure their survival in nutrient-limited systems
512 (Salem et al., 2006). The decay rates of DPAOs in AS_{ANA.end} and AS_{AER.end} did not
513 appreciably differ in the present study.

514 **4.3. Recovery of nitrite/nitrate-DPAOs activities**

515 Transition from starvation to full functionality is essential for the survival of bacterial
516 systems (Lu et al. 2007). Vargas et al. (2013) found that once wastewater is
517 reintroduced, both PAOs and GAOs can recover their initial acetate uptake rates,
518 indicating strong survival ability during the starvation period. Yilmaz et al (2007) also
519 reported that the P-release and P-uptake in a starved culture were fully recovered
520 within 4 days of gradual re-introduction of influent wastewater. In the present study,
521 nitrite-DPAOs recovered from 12-day starvation within one day (Figure 5). These

522 findings well correspond with the lower maintenance energy requirement and decay
523 rate in nitrite-DPAO sludges than those in nitrate-DPAO sludges. In particular, for the
524 nitrite-DPAOs sludge, less (about 40%) PHA consumption for anoxic P uptake as
525 well as high PHA synthesis during the endogenous period than that of the
526 nitrate-DPAOs sludge (Table 3) may speed up their anoxic metabolism during the
527 recovery period, which thus provides an additional benefit to the stable operation of
528 shortcut denitrification P removal systems.

529 Microorganisms in $AS_{ANA,end}$ rapidly recovered their intracellular polymer
530 transformation ability, especially for the nitrite-DPAOs in $A-R_{NO_2-}$, where glycogen
531 synthesis and PHA degradation reached 179% and 99%, respectively, of their
532 pre-starvation levels (Figure 5g and Figure S1f). This observation is consistent with
533 the strong recovery of denitrifying P removal efficiency with the value of 136%
534 (Table 4), indicating a high activity of nitrite-DPAOs. The post-starvation nitrate
535 reduction rate in $A-R_{NO_3-}$ was approximately 35% less than the pre-starvation rate.
536 Since no external carbon was added in the anoxic phase during the first recovery
537 batch test, OHOs could not have been involved in nitrite/nitrate reduction. Thus,
538 nitrate denitrification was accomplished by PAOI and/or DGAOs (Zeng et al., 2003b).
539 PAOI can simultaneously reduce nitrate and remove anoxic P, but PAOII cannot use
540 nitrate as an electron acceptor (Flowers et al., 2009). Therefore, the reduced nitrate
541 denitrification rates suggest that starvation shock may inhibit the activity of PAOI
542 and/or DGAOs.

543 The metabolism of intracellular materials in AS_{AER.end} was severely inhibited by
544 long-term starvation, as evidenced by the decrease in P uptake and release. Conversely,
545 both reactors achieved complete denitrification, probably because the abundant
546 propionate (2.89 and 3.22 mmol C/L for O-R_{NO3-} and O-R_{NO2-}, respectively) derived
547 from the preceding anaerobic phase stimulated the denitrification performance of
548 OHOs. However, the low effluent P concentration in O-R_{NO2-} confirmed that a fully
549 functional system could be restored by the relatively high fraction of PAOII (Table 1).

550 In summary, the relatively low consumption of intracellular polymers, slow cell
551 decay and rapid recovery of activity in nitrite-DPAO sludges (especially originating
552 from the anaerobic end phase of the DPR process) demonstrate a strong ability to
553 cope with starvation shock. These endogenous process characteristics of nitrite-DPAO
554 sludges, combined with 25% reduction in the oxidation cost and 40% reduction in
555 carbon consumption, may be exploited in efficient shortcut denitrification P removal.

556 5. Conclusions

557 (1) The anaerobic maintenance energy was approximately 30% lower in
558 nitrite-DPAOs sludge than that in nitrate-DPAOs sludge. Glycogen and poly-P
559 sequentially served as the primary maintenance energy sources in starved
560 nitrite/nitrate-DPAOs. The polysaccharides in EPS were rapidly consumed by
561 nitrate-DPAOs sludge during the first 3 days of starvation; conversely, nitrite-DPAOs
562 sludge converted less of these polysaccharides into maintenance energy.

563 (2) The estimated cell decay rates in A-R_{NO3-}, O-R_{NO3-}, A-R_{NO2-} and O-R_{NO2-} were

564 0.022, 0.022, 0.008, and 0.007 day⁻¹, respectively. Clearly, the cell decay rates were
565 lower in nitrite-DPAOs than those in nitrate-DPAOs, indicating a better stringent
566 starvation response by nitrite-cultivated DPAOs than by their nitrate-cultivated
567 counterparts.

568 (3) After 12 days of starvation, nitrite-DPAO sludges recovered more rapidly than
569 nitrate-DPAO sludges. The denitrifying P removal efficiencies, as well as the
570 transformation rates of intracellular polymers in the nitrite-DPAO sludges (especially
571 that from the end of the anaerobic phase) were almost identical to their pre-starvation
572 values, indicating a rapid return (within 1 day) to full functionality.

573 **Acknowledgements**

574 This study was supported by the National Natural Science Foundation of China
575 (NSFC) (nos. 51178325 and 51378370), the Shanghai Science and Technology
576 Committee Rising-Star Tracking Program (12QH1402400) and the Fundamental
577 Research Funds for Central Universities (Tongji University) (0400219238).

578 **References**

- 579 Abeling, U., Seyfried, C.F., 1992. Anaerobic-aerobic treatment of high-strength ammonium
580 wastewater nitrogen removal via nitrite. *Water Sci. Technol.* 26 (5–6), 1007–1015.
- 581 APHA, 1998. *Standard Methods for the Examination of Water and Wastewater*, twentieth ed.
582 American Public Health Association, Washington D.C., USA.
- 583 Carvalho, G., Lemos, P.C., Oehmen, A., Reis, M.A., 2007. Denitrifying phosphorus removal:
584 linking the process performance with the microbial community structure. *Water Res.* 41 (19),

- 585 4383–4396.
- 586 Flemming, H. C., Wingender, J. 2010. The biofilm matrix. *Nat. Rev. Microbiol.*, 8 (9), 623–633.
- 587 Flowers, J. J., He, S., Yilmaz, S., Noguera, D. R., McMahon, K.D., 2009. Denitrification
- 588 capabilities of two biological phosphorus removal sludges dominated by different *Candidatus*
- 589 *Accumulibacter* clades. *Environ. Microbiol. Rep.* 1 (6), 583–588.
- 590 Filipe, C. D., Daigger, G. T., Grady, C. P., 2001. A metabolic model for acetate uptake under
- 591 anaerobic conditions by glycogen accumulating organisms: stoichiometry, kinetics, and the
- 592 effect of pH. *Biotechnol. Bioeng.* 76 (1), 17–31.
- 593 Guisasola, A., Quirie, M., Vargas, M. D., Casas, C., Baeza, J. A., 2009. Failure of an enriched
- 594 nitrite-DPAO population to use nitrate as an electron acceptor. *Process Biochem.* 44, 689–695.
- 595 Hao, X., Wang, Q., Cao, Y., van Loosdrecht, M., 2010 (a). Experimental evaluation of decrease in
- 596 the activities of polyphosphate/glycogen-accumulating organisms due to cell death and activity
- 597 decay in activated sludge. *Biotechnol. Bioeng.* 106 (3), 399–407
- 598 Hao, X., Wang, Q., Zhu, J., Van Loosdrecht, M.C., 2010 (b). Microbiological endogenous
- 599 processes in biological wastewater treatment systems. *Crit. Rev. Env. Sci. Tec.* 40 (3), 239–
- 600 265.
- 601 Kaplan, J. B., Velliyagounder, K., Rangunath, C., Rohde, H., Mack, D., Knobloch, J. K. M.,
- 602 Ramasubbu, N., 2004. Genes involved in the synthesis and degradation of matrix
- 603 polysaccharide in *Actinobacillus actinomycetemcomitans* and *Actinobacillus*
- 604 *pleuropneumoniae* biofilms. *J. Bacteriol.*, 186 (24), 8213–8220.
- 605 Laue, H., Schenk, A., Li, H., Lambertsen, L., Neu, T. R., Molin, S., Ullrich, M. S., 2006.

- 606 Contribution of alginate and levan production to biofilm formation by *Pseudomonas*
607 *syringae*. *Microbiology*, 152 (10), 2909–2918.
- 608 Lesouef, A., Payraudeau, M., Rogalla, F., Kleiber, B., 1992. Optimizing nitrogen removal reactor
609 configurations by on-site calibration of the IAWPRC activated sludge model. *Water Sci.*
610 *Technol.* 25 (6), 105–123.
- 611 Lopez, C., Pons, M.N., Morgenroth, E., 2006. Endogenous processes during long-term starvation
612 in activated sludge performing enhanced biological phosphorus removal. *Water Res.* 40 (8),
613 1519–1530.
- 614 Lu, H., Keller, J., Yuan, Z., 2007. Endogenous metabolism of *Candidatus Accumulibacter*
615 *phosphatis* under various starvation conditions. *Water Res.* 41 (20), 4646–4656.
- 616 Marcelino, M., Wallaert, D., Guisasola, A., Baeza, J.A., 2011. A two-sludge system for
617 simultaneous biological C, N and P removal via the nitrite pathway. *Water Sci. Technol.* 64 (5),
618 1142–1147.
- 619 Martín, H. G., Ivanova, N., Kunin, V., Warnecke, F., Barry, K.W., McHardy, A.C., Yeates, C., He,
620 S., Salamov, A.A., Szeto, E., 2006. Metagenomic analysis of two enhanced biological
621 phosphorus removal (EBPR) sludge communities. *Nat. Biotechnol.* 24 (10), 1263–1269.
- 622 Miyake, H., Morgenroth, E., 2005. Optimization of enhanced biological phosphorus removal after
623 periods of low loading. *Water Environ. Res.* 77 (2), 117–127.
- 624 Morgenroth, E., Obermayer, A., Arnold, E., Brl, A., Wagner, M., Wilderer, P., 2000. Effect of
625 long-term idle periods on the performance of sequencing batch reactors. *Water Sci. Technol.*
626 41 (1), 105–113.

- 627 Murnleitner, E., Kuba, T., van Loosdrecht, M. C. M., Heijnen, J. J., 1997. An integrated metabolic
628 model for the aerobic and denitrifying biological phosphorus removal. *Biotechnol. Bioeng.* 54
629 (5), 434–450.
- 630 Oehmen, A., Zeng, R.J., Saunders, A.M., Blackall, L.L., Keller, J., Yuan, Z., 2006. Anaerobic and
631 aerobic metabolism of glycogen-accumulating organisms selected with propionate as the sole
632 carbon source. *Microbiology.* 152 (9), 2767–2778.
- 633 Oehmen, A., Zeng, R.J., Yuan, Z., Keller, J., 2005. Anaerobic metabolism of propionate by
634 polyphosphate-accumulating organisms in enhanced biological phosphorus removal systems.
635 *Biotechnol. Bioeng.* 91 (1), 43–53.
- 636 Salem, S., Moussa, M.S., Van Loosdrecht, M., 2006. Determination of the decay rate of nitrifying
637 bacteria. *Biotechnol. Bioeng.* 94 (2), 252–262.
- 638 Smolders, G., Van der Meij, J., Van Loosdrecht, M., Heijnen, J.J., 1994. Stoichiometric model of
639 the aerobic metabolism of the biological phosphorus removal process. *Biotechnol. Bioeng.* 44
640 (7), 837–848.
- 641 Smolders, G., Van Loosdrecht, M., Heijnen, J.J., 1995. A metabolic model for the biological
642 phosphorus removal process. *Water Sci. Technol.* 31 (2), 79–93.
- 643 Tayà, C., Garlapati, V.K., Guisasola, A., Baeza, J.A., 2013. The selective role of nitrite in the
644 PAO/GAO competition. *Chemosphere.* 93 (4), 612–618.
- 645 Vargas, M., Yuan, Z., Pijuan, M., 2013. Effect of long-term starvation conditions on
646 polyphosphate-and glycogen-accumulating organisms. *Bioresour. Technol.* 127, 126–131.
- 647 Wang, Q., Ye, L., Jiang, G., Yuan, Z., 2013a. A free nitrous acid (FNA)-based technology for

- 648 reducing sludge production. *Water Res.* 47 (11), 3663–3672.
- 649 Wang, Y., Geng, J., Ren, Z., He, W., Xing, M., Wu, M., Chen, S., 2011. Effect of anaerobic
650 reaction time on denitrifying phosphorus removal and N₂O production. *Bioresour. Technol.*
651 102 (10), 5674–5684.
- 652 Wang, Y., Geng, J., Peng, Y., Wang, C., Guo, G., Liu, S., 2012. A comparison of endogenous
653 processes during anaerobic starvation in anaerobic end sludge and aerobic end sludge from an
654 anaerobic/anoxic/oxic sequencing batch reactor performing denitrifying phosphorus removal.
655 *Bioresour. Technol.* 104, 19–27.
- 656 Wang, Y., Guo, G., Wang, H., Stephenson, T., Guo, J., Ye, L., 2013b. Long-term impact of
657 anaerobic reaction time on the performance and granular characteristics of granular
658 denitrifying biological phosphorus removal systems. *Water Res.* 47 (14), 5326–5337.
- 659 Wang, Z., Liu, Y., Tay, J., 2005. Distribution of EPS and cell surface hydrophobicity in aerobic
660 granules. *Appl. Microbiol. Biot.* 69 (4), 469–473.
- 661 Wang, Z., Liu, Y., Tay, J., 2007. Biodegradability of extracellular polymeric substances produced
662 by aerobic granules. *Appl. Microbiol. Biot.* 74 (2), 462–466.
- 663 Yagci, N., Artan, N., Çokgör, E.U., Randall, C.W., Orhon, D., 2003. Metabolic model for acetate
664 uptake by a mixed culture of phosphate-and glycogen-accumulating organisms under
665 anaerobic conditions. *Biotechnol. Bioeng.* 84 (3), 359–373.
- 666 Yilmaz, G., Lemaire, R., Keller, J., Yuan, Z., 2007. Effectiveness of an alternating aerobic,
667 anoxic/anaerobic strategy for maintaining biomass activity of BNR sludge during long-term
668 starvation. *Water Res.* 41 (12), 2590–2598.

- 669 Zeng R.J., Van Loosdrecht, M., Yuan Z.G., Keller J., 2003a. Metabolic model for
670 glycogen-accumulating organisms in anaerobic/aerobic activated sludge systems. *Biotechnol.*
671 *Bioeng.* 81(1), 92–105.
- 672 Zeng, R. J., Yuan, Z., Keller, J., 2003b. Enrichment of denitrifying glycogen-accumulating
673 organisms in anaerobic/anoxic activated sludge system. *Biotechnol. Bioeng.* 81 (4), 397–404.
- 674 Zhang, X., Bishop, P.L., 2003. Biodegradability of biofilm extracellular polymeric substances.
675 *Chemosphere.* 50 (1), 63–69.
- 676 Zhou, Y., Oehmen, A., Lim, M., Vadivelu, V., Ng, W. J., 2011. The role of nitrite and free nitrous
677 acid (FNA) in wastewater treatment plants. *Water Res.* 45 (15), 4672–4682.
678
679

680 **Figure captions**

681 **Fig. 1.** Variations in (a) NH_4^+ -N and (b) PO_4^{3-} -P concentrations in A- $\text{R}_{\text{NO}_3^-}$, O- $\text{R}_{\text{NO}_3^-}$,
682 A- $\text{R}_{\text{NO}_2^-}$, and O- $\text{R}_{\text{NO}_2^-}$ during the 12 days of anaerobic starvation.

683 **Fig. 2.** Variations in (a) MLSS, (b) MLVSS, and (c) MLVSS/MLSS ratio in A- $\text{R}_{\text{NO}_3^-}$,
684 O- $\text{R}_{\text{NO}_3^-}$, A- $\text{R}_{\text{NO}_2^-}$, and O- $\text{R}_{\text{NO}_2^-}$ during the 12 days of anaerobic starvation.

685 **Fig. 3.** Variations in glycogen and PHA during the 12 days of anaerobic starvation: (a),
686 A- $\text{R}_{\text{NO}_3^-}$, (b), O- $\text{R}_{\text{NO}_3^-}$, (c), A- $\text{R}_{\text{NO}_2^-}$, and (d), O- $\text{R}_{\text{NO}_2^-}$.

687 **Fig. 4.** EPS contents profile during the 12 days of anaerobic starvation in A- $\text{R}_{\text{NO}_3^-}$,
688 O- $\text{R}_{\text{NO}_3^-}$, A- $\text{R}_{\text{NO}_2^-}$, and O- $\text{R}_{\text{NO}_2^-}$: (a) proteins, (b) polysaccharides, and (c) EPS
689 (calculated as the sum of proteins, polysaccharides and humics). Data are the averages
690 and their standard deviations in triplicate tests.

691 **Fig. 5.** Variations in NO_x^- -N, PO_4^{3-} -P, glycogen and PHA in the recovery batch tests
692 after 12 days of anaerobic starvation: (a), (e), A- $\text{R}_{\text{NO}_3^-}$; (b), (f), O- $\text{R}_{\text{NO}_3^-}$; (c), (g),
693 A- $\text{R}_{\text{NO}_2^-}$; and (d), (h), O- $\text{R}_{\text{NO}_2^-}$.

694 **Fig. 6.** ATP production profile during the 12 days of anaerobic starvation: (a), A- $\text{R}_{\text{NO}_3^-}$,
695 (b), O- $\text{R}_{\text{NO}_3^-}$, (c), A- $\text{R}_{\text{NO}_2^-}$, and (d), O- $\text{R}_{\text{NO}_2^-}$.

696

697

698
699
700
701**Table 1.** Comparison of the anaerobic carbon transformations, PO_4^{3-} -P release, and biomass compositions (\pm standard error) with propionate supplied as carbon source in a typical cycle

	FISH quantification					PO_4^{3-} -P / VFA ^f	Gly/ VFA ^g	PHA/ VFA ^g	PHB/ VFA ^g	PHV/ VFA ^g	PH2MV/ VFA ^g
	Ac_{Tot} ^a (%)	Ac_I ^b (%)	Ac_{II} ^c (%)	De ^d (%)	Co ^e (%)						
This study											
SBR _{NO3} (nitrate-based)	66 ± 1.5	28 ± 1.9	38 ± 1.4	27 ± 0.9	<1	0.32	0.44	1.54	0.08	0.66	0.80
SBR _{NO2} (nitrite-based)	75 ± 1.1	21 ± 1.2	54 ± 1.7	19 ± 0.6	<1	0.36	0.31	1.46	0.11	0.61	0.74
Previous studies											
Oehmen et al. (2005)	63 ± 1.3	-	-	<1	<1	0.42	0.32	1.23	0.04	0.55	0.65
Carvalho et al. (2007)	75	44	31	<1	<1	0.40	0.32	0.97	0	0.40	0.57
Tayà et al. (2013)	85	55	30	-	<10	0.34	0.49	1.47	-	-	-

^a Ac_{Tot} : Total *Accumulibacter*. ^b Ac_I : Type I *Accumulibacter*. ^c Ac_{II} : Type II *Accumulibacter*. ^d De : *Defluvicoccus*. ^e Co : *Competibacter*.

^fUnits PO_4^{3-} -P mmol/C mmol. ^gUnits C mmol/C mmol. - No data.

Table 2. Comparison of cell decay of PAOs/DPAOs in this study and previous studies during the 12 days of anaerobic starvation.

	Starvation condition	Initial MLVSS (g/L)	Temperature (°C)	Starvation period (d)	SRT (d)	NH ₄ ⁺ -N release (mg/L)	Cell decay rate (1/d)
This study							
A-R _{NO3-}						41.8 ^a	0.022 ^a
O-R _{NO3-}	anaerobic	2.5	20 ± 2	12	20	39.5 ^b	0.022 ^b
A-R _{NO2-}						18.7 ^a	0.008 ^a
O-R _{NO2-}						15.8 ^b	0.007 ^b
Previous studies							
Lu et al. (2007)	anaerobic	1.6	22 ± 2	8	24	3.2 ^b	0.006 ^b (day 4– 8)
Hao et al. (2010a)	anaerobic	-	22 ± 0.5	7	12	-	0.036 ± 0.003 ^b
Wang et al. (2012)	anaerobic	2.4	10 – 15	7	20	1.12 ^a 1.59 ^b	0.0006 ^a 0.0008 ^b
Vargas et al. (2013)	aerobic-anaerobic	2.6	20 ± 2	21	46.8	14 ^b	0.029 ^b

^a All results represent the sludge from the anaerobic end phases.

^b All results represent the sludge from the aerobic end phases.

702

Table 3. Transformations of materials in the liquid- and solid-phase in A-R_{NO3-}, O-R_{NO3-}, A-R_{NO2-} and O-R_{NO2-} during the 12 days of anaerobic starvation.

Parameters	Nitrate-sludge		Nitrite-sludge	
	A-R _{NO3-}	O-R _{NO3-}	A-R _{NO2-}	O-R _{NO2-}
MLSS reduction (mg/L)	770	1650	670	910
MLVSS reduction (mg/L)	357	793	360	347
PO ₄ ³⁻ -P release (mg/L)	87.2	150.8	45.3	102.7
Glycogen degradation (mmol-C/g-MLVSS)	3.03	5.56	2.41	3.44
Glycogen degradation rate ^a (mmol-C/g-MLVSS/d)	0.61	1.11	0.48	0.69
PHB synthesis (mmol-C/g-MLVSS)	0.23 (0.12)	0.58 (0.19)	0.19 (0.07)	0.54 (0.15)
PHV synthesis (mmol-C/g-MLVSS)	1.07 (0.58)	1.42 (0.46)	1.16 (0.42)	1.40 (0.39)
PH2MV synthesis (mmol-C/g-MLVSS)	0.54 (0.29)	1.06 (0.35)	1.44 (0.52)	1.66 (0.46)
PHA synthesis (mmol-C/g-MLVSS)	1.84	3.06	2.79	3.61
PHA synthesis rate (mmol-C/g-MLVSS/d)	0.30 ^a	0.58 ^a	0.76 ^b	1.02 ^b
Polysaccharides consumption (mg/g-MLVSS)	36.6 ± 0.4	46.4 ± 0.5	11.7 ± 0.8	10.1 ± 0.4
Proteins consumption (mg/g-MLVSS)	144.0 ± 2.3	129.0 ± 13.3	133.1 ± 9.3	146.8 ± 1.5
Total EPS consumption (mg/g-MLVSS)	196.0 ± 0.1	200.1 ± 9.0	162.4 ± 0.3	177.6 ± 7.2

^a All results obtained during the first 5 days.^b All results obtained during the first 3 days.

Data in the brackets represent the fractions of the components in PHA.

703

704

705

Table 4. Comparison of denitrifying P-removal efficiency during anaerobic/anoxic phases in typical cycles and recovery batch tests.

Items	Amount of PO_4^{3-} -P release ^a	Amount of PO_4^{3-} -P uptake ^a	Amount of NO_x -N reduction ^b	P/N ratio
Nitrate-sludge				
SBR _{NO3-}	52.33	36.69	33.37	1.10
A-R _{NO3-}	47.98 (91.7) *	19.37 (52.8)	19.36 (58.0)	1.00 (63.7)
O-R _{NO3-}	6.87 (13.1)	4.09 (11.1)	33.68 (100.9)	0.12 (7.6)
Nitrite-sludge				
SBR _{NO2-}	57.48	26.44	33	0.80
A-R _{NO2-}	47.30 (82.3) *	35.97 (136.0)	30 (90.9)	1.20 (69.0)
O-R _{NO2-}	11.82 (20.6)	5.73 (21.7)	33 (100.0)	0.17 (9.8)

706 ^a Units mg PO_4^{3-} -P/L.707 ^b Units mg NO_x -N/L.

708 * Results obtained from the second recovery batch tests.

709 Data in brackets represent the percentage recovery relative to values obtained in typical cycles of
710 the corresponding parent SBRs (%).

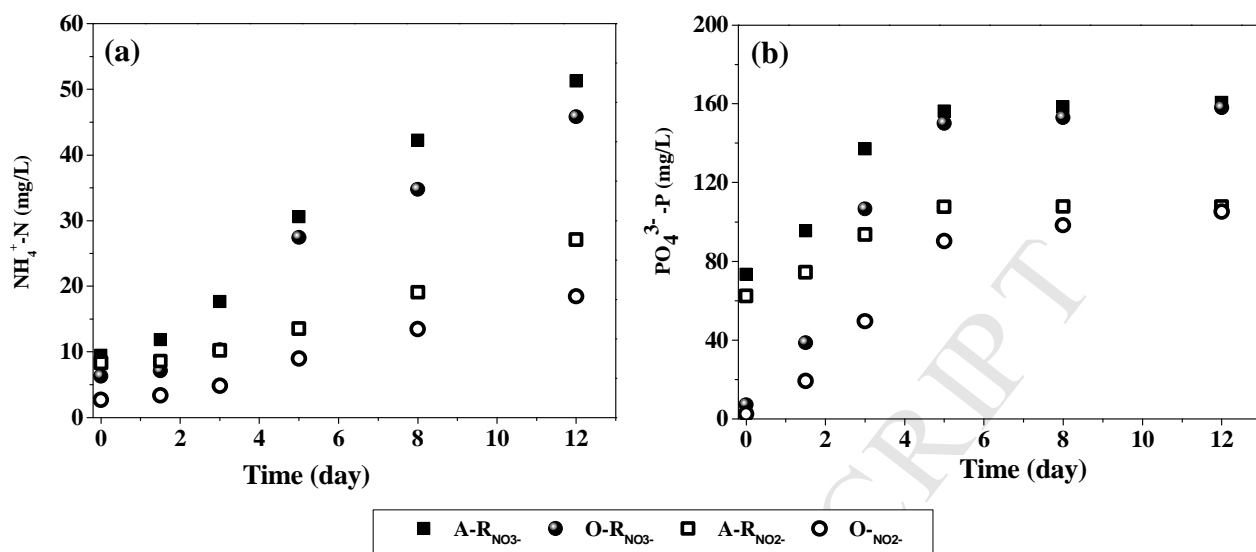
711

712

713

714

715 Fig. 1

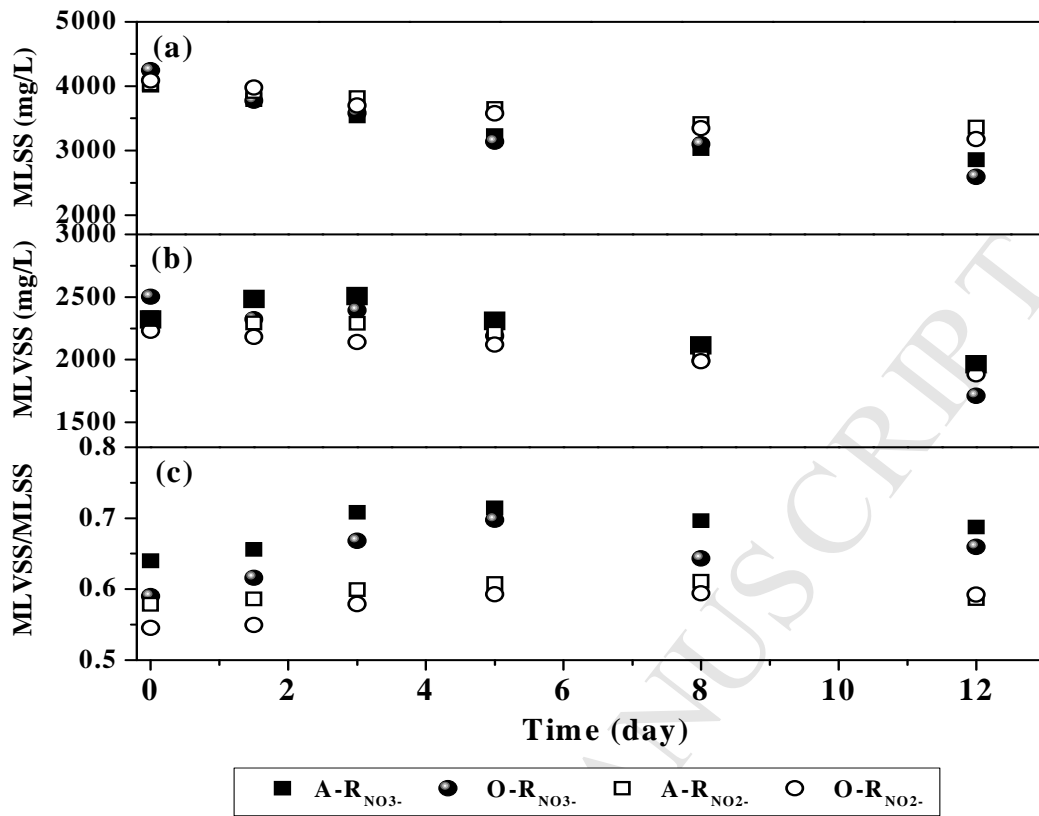


716

717

718

719 Fig. 2



720

721

722

723

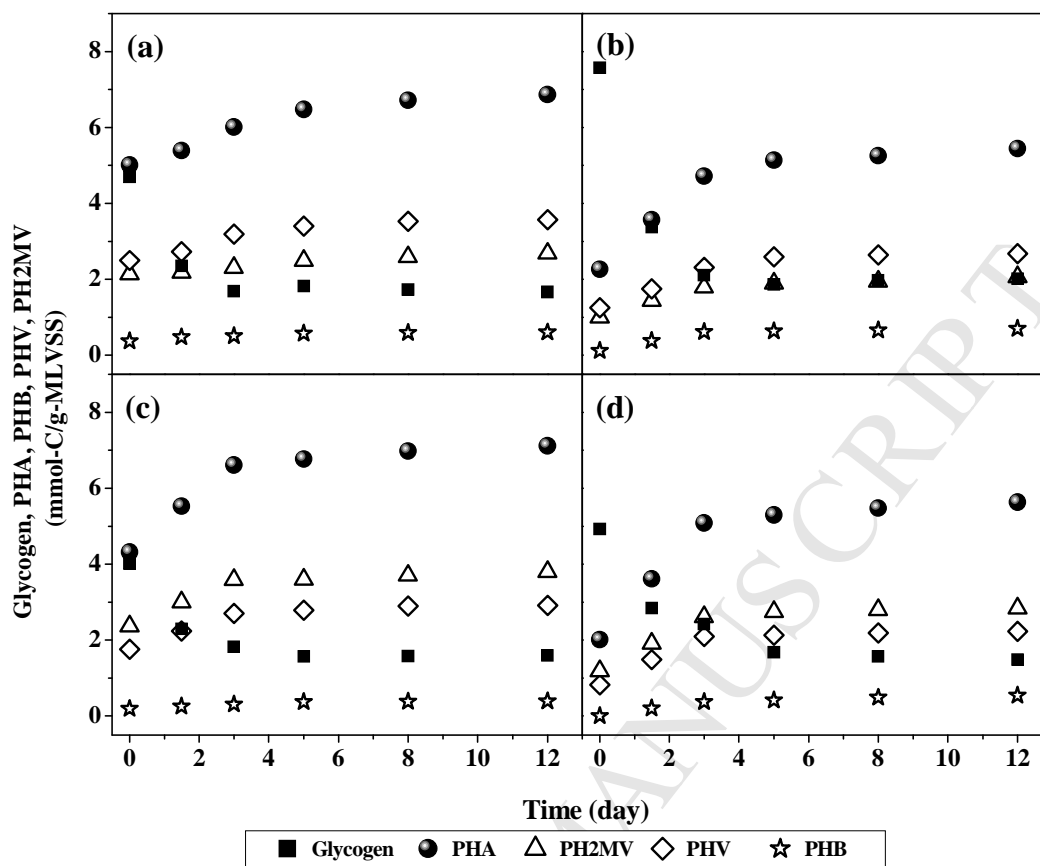
724

725

726

727

728 Fig. 3

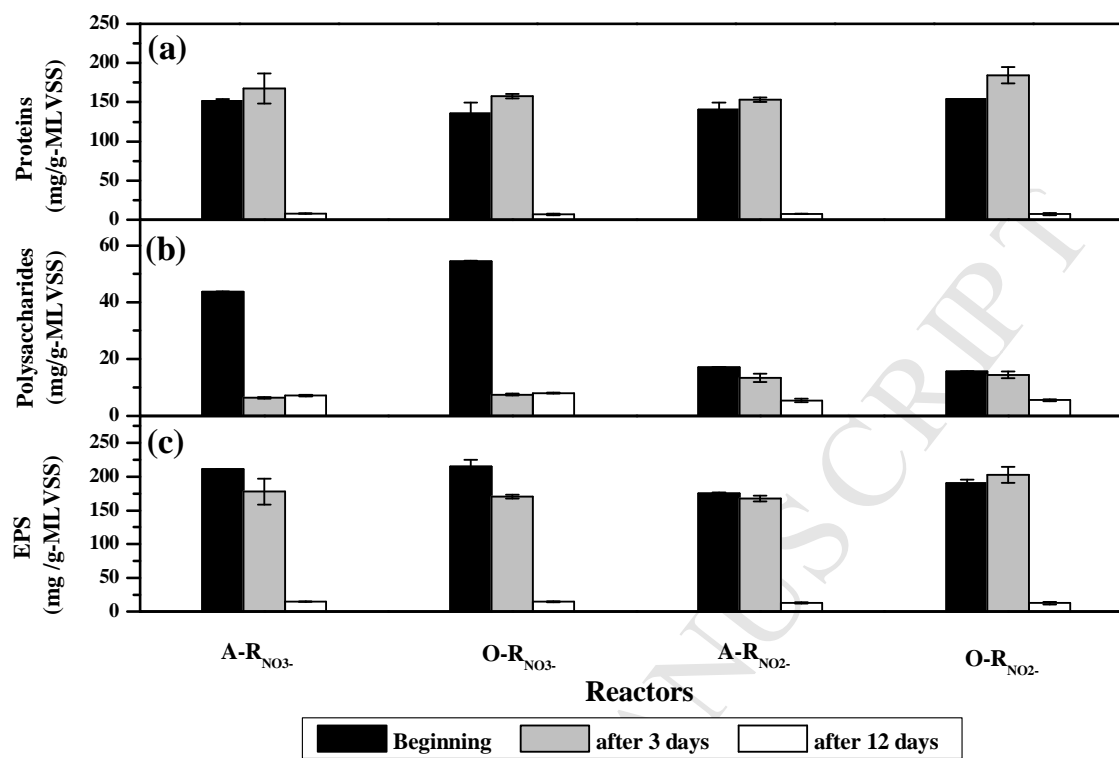


729

730

731

732

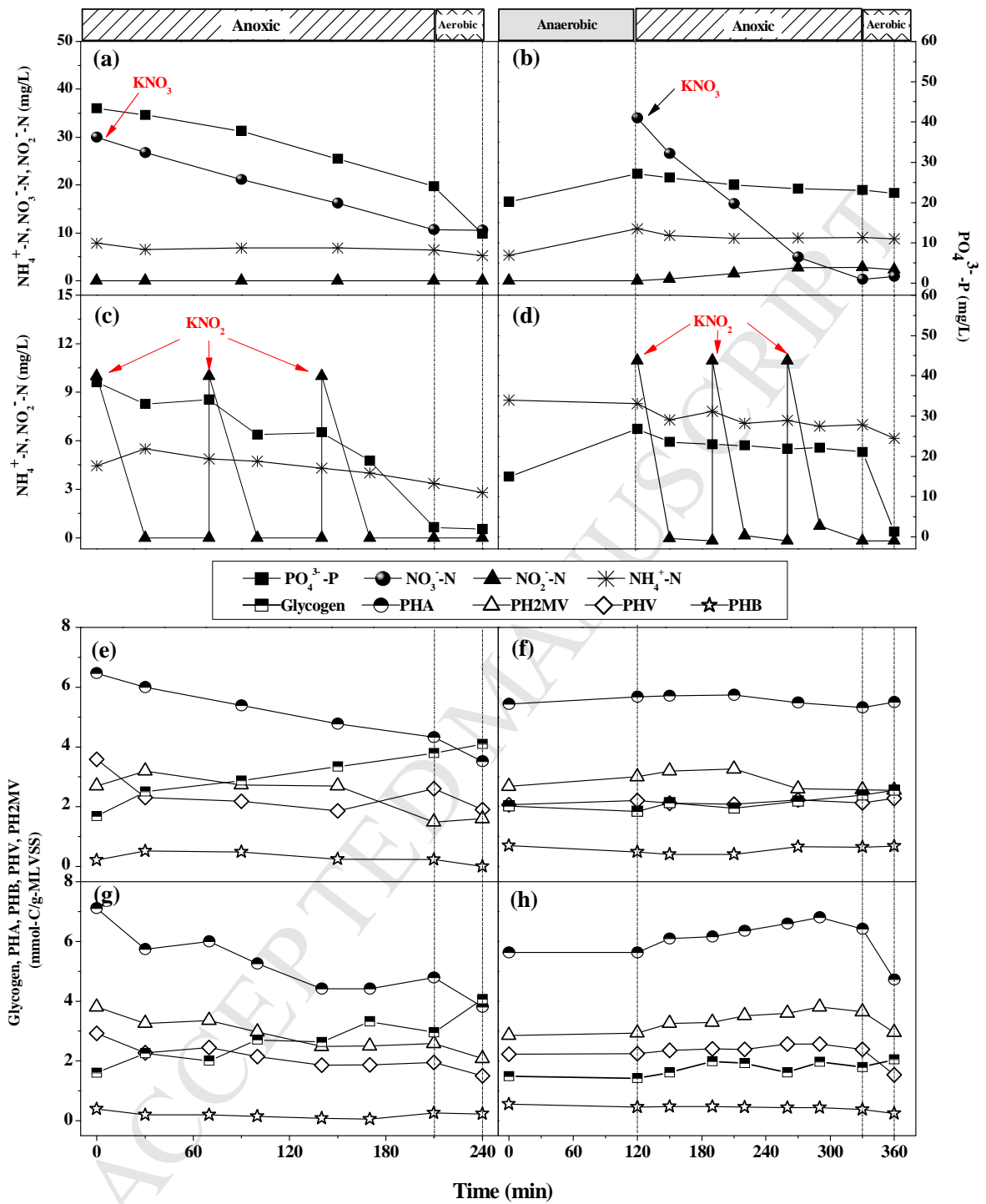
733 **Fig. 4**

734

735

736

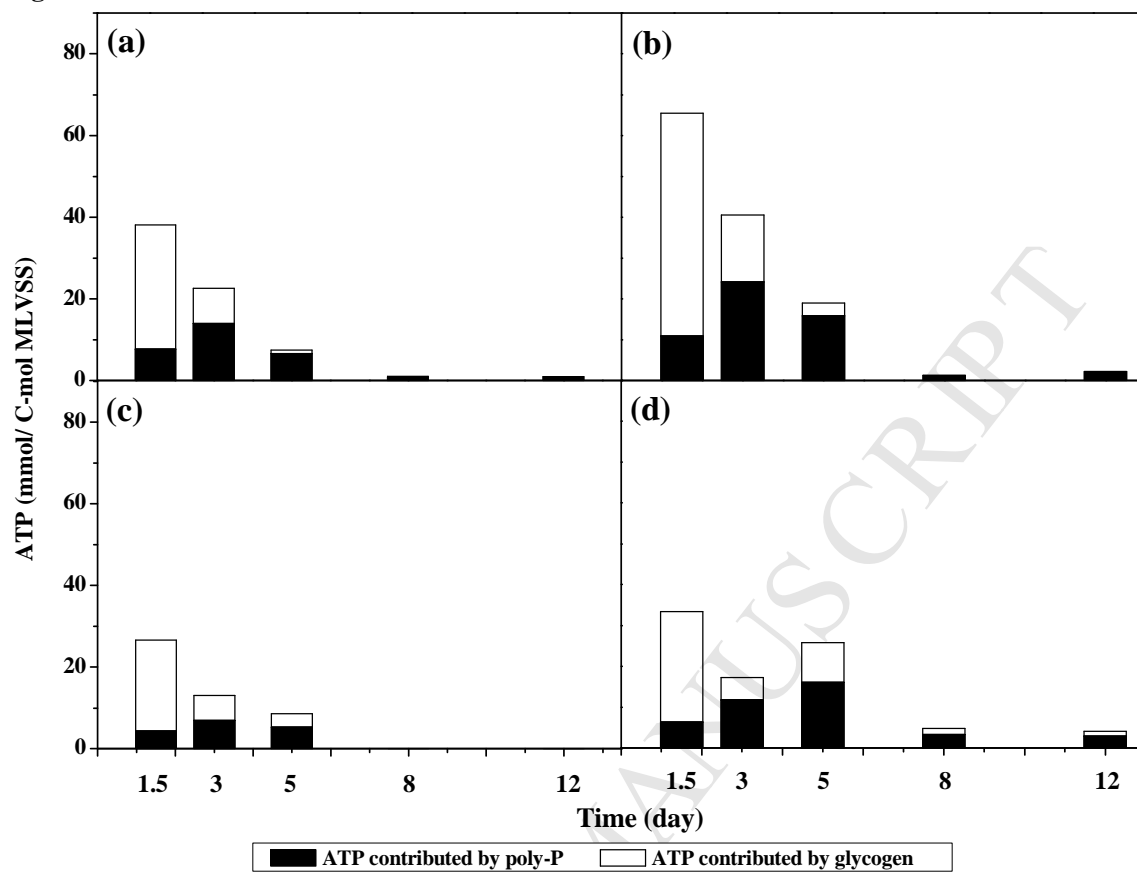
737 Fig. 5



738

739

740

741 **Fig. 6**

742

743

744

745

746 **Supplementary Information**

747

748 **Title: Comparison of endogenous metabolism during long-term anaerobic**
749 **starvation of nitrite/nitrate cultivated denitrifying phosphorus removal sludges**

750

751 Yayi Wang^{1*}, Shuai Zhou¹, Hong Wang¹, Liu Ye², Jian Qin¹, Ximao Lin¹

752 *Corresponding author. Tel: +21 65984275; Fax: +21 65984275; E-mail:

753 yayi.wang@tongji.edu.cn

754

755 ¹State Key Laboratory of Pollution Control and Resources Reuse, College of

756 Environmental Science and Engineering, Tongji University, Siping Road, Shanghai

757 200092, P. R. China

758 ²School of Chemical Engineering, The University of Queensland, St Lucia, Brisbane

759 4072, Australia

760

761 **Text S1. The detailed descriptions of analysis of VFA, PHA, glycogen, and EPS**762 **a) VFA**

763 VFA (propionate) was measured using an Agilent 6890N gas chromatograph (GC)

764 equipped with a 30 m×0.53 mm×1 μm (length×ID×film) DB-WAXetr column and a

765 flame ionization detector (FID) at 220 °C.

766 **b) PHA**

767 PHA, including poly- β -hydroxybutyrate (PHB), poly- β -hydroxyvalerate (PHV),
768 poly-3-hydroxy-2-methylvalerate (PH2MV), was measured according to a method
769 described by Oehmen et al. (2005). Briefly, approximately 20 mg freeze-dried
770 samples of biomass were put into screw-topped glass tubes, and 2 mL of chloroform,
771 2 mL of an acidified methanol solution (10% H₂SO₄) and 0.1 mL benzoic acid
772 methanol solution (2 g of benzoic acid dissolved in 100 mL methanol used as an
773 internal standard) were subsequently added. The samples were then digested for 4 h at
774 100 °C. After cooling, 1 mL of distilled water was added and mixed vigorously with
775 each sample. Thereafter, 1 h of settling time was allowed to achieve phase separation.
776 When the phases were separated, approximately 1 mL of the bottom organic layer was
777 transferred to the GC vials for analysis. 3 μ L of the chloroform phase was analyzed
778 with a gas chromatograph (Thermo Focus GC). The chromatograph was operated with
779 a HP-5 column (30 m length \times 0.32 mm ID \times 0.25 μ m film), a split injection ratio of
780 1:15 and helium as the carrier gas (1.5 mL/min). A flame ionisation detection (FID)
781 unit was operated at 250 °C with an injection port temperature of 230 °C. The oven
782 temperature was set to 80 °C for 4 min, increased at 8 °C /min to 120 °C, and then to
783 220 °C at 30 °C /min and held for 2 min.

784 **c) Glycogen**

785 Glycogen was determined by the anthrone method (Frølund et al., 1996). A 5-ml
786 volume of 0.6 M HCl was added to weighed (approximately 10 mg), freeze-dried
787 biomass in screw-topped glass tubes, and then heated at 100 °C for 3 h. After cooling

788 to room temperature, samples were sheared by a vortex mixer (XW-80A,
789 Shanghai Qingpu Huxi Instrument Co., Ltd, China) for 1 min, and were transferred to
790 10-mL tubes, followed by centrifugation (CT15RT, Techcomp, China) for 5 min at
791 10 000 g. About 1 mL supernatant was added to 4 mL of anthrone-H₂SO₄ reagent (0.2%
792 anthrone (w/v) in 80% (v/v) H₂SO₄) in 10-mL colorimetric tubes. All tubes were
793 placed in a water bath at 100 °C for 10 min. After cooling at 4 °C for 5 min in cold
794 water, samples were measured by a UV/VIS spectrophotometer (UV765, Shanghai
795 Precision & Scientific Instrument Co., Ltd, China) at 625 nm. Glucose was used as
796 the standard.

797 **d) EPS**

798 A heat extraction method (Li et al., 2007) was applied to extract the EPS (including
799 loosely bound EPS (LB-EPS) and tightly bound EPS (TB-EPS)) in the sludge. 30 mL
800 sludge suspension was first dewatered by centrifugation (CT15RT, Techcomp, China)
801 in a 50-mL tube at 4 000 g for 5 min. The supernatant was recovered for water quality
802 analysis. The sludge pellet in the tube was re-suspended into 15 mL of 0.05% NaCl
803 solution. The sludge mixture was then diluted with the NaCl solution (pre-heating to
804 70 °C) to its original volume of 30 mL. Immediately, the sludge suspension was
805 sheared by a vortex mixer (XW-80A, Shanghai Qingpu Huxi Instrument Factory,
806 China) for 1 min, followed by centrifugation at 4 000 g for 10 min. The organic
807 matter in the supernatant was readily extractable EPS, and was regarded as the
808 LB-EPS of the biomass. For the extraction of the TB-EPS, the sludge pellet left in the

809 centrifuge tube was re-suspended in 0.05% NaCl solution to its original volume of 30
810 mL. The sludge suspension was heated to 60 °C in a water bath for 30 min. After
811 cooling to room temperature, the sludge mixture was centrifuged at 4 000 g for 15
812 min. The supernatant collected was regarded as the TB-EPS of the sludge.

813 Both the LB-EPS and TB-EPS extractions were analyzed for proteins (PN),
814 polysaccharides (PS) and humic-like substances (HS). The PN and HS were analyzed
815 by a UV/VIS spectrophotometer (UV765, Shanghai Precision & Scientific Instrument
816 Co., Ltd, China) following the modified Lowry method (Frølund et al., 1995) using
817 bovine serum albumin (Sigma) and humic acid (Fluka) as the standards, respectively.
818 The PS content was determined by the anthrone method described by Frølund et al.
819 (1996) using glucose as the standard.
820

821 **Text S2. Fluorescent in situ hybridization (FISH)**

822 Fluorescence in situ hybridization (FISH) was performed as described by Amann
823 (1995) using Cy5-labelled EUBMIX probes, which are specific for most Bacteria
824 (Daims et al., 1999). The Cy3-labelled PAOMIX probe (PAO462, PAO651 and
825 PAO846) were used to target *Candidatus Accumulibacter phosphatis* (Crocetti et al.,
826 2000), a known PAO; the Cy3-labelled GAOMIX probe (GAOQ431, GAOQ989 and
827 GB_G2), DFMIX probe (TFO_DF 218 and TFO_DF 618, and DF 988 and DF 1020)
828 were used to target *Candidatus Competibacter phosphatis*, *Defluvicoccus*-related TFO
829 (Cluster I) in *Alphaproteobacteria*, and *Defluvicoccus*-related DF (Cluster II) in
830 *Alphaproteobacteria* (Crocetti et al., 2002; Kong et al., 2002; Wong et al., 2004) to
831 determine the microbial population distributions of the PAOs and GAOs (Table S1).
832 All oligonucleotide probes were commercially synthesized, and all hybridization
833 buffer contained 35% (v/v) formamide. Cy5-labeled Acc-I-444 was used to target
834 PAOI *Accumulibacter*, while FAM-labeled Acc-II-444 was used to target PAOIIA,
835 IIC and IID *Accumulibacter* (Flowers et al. 2009).

836 FISH preparations were visualized using a Zeiss LSM 510 Meta confocal
837 laser-scanning microscope (CLSM) using a Plan-Apochromat 63×oil (NA1.4)
838 objective. Thirty images were taken from each sample for quantification. The
839 percentage of *Accumulibacter*, *Competibacter* and *Defluvicoccus* in the entire
840 bacterial population (EUBMIX) was determined via FISH image analysis using image
841 analyzing software (Image-Pro Plus, V6.0, Media Cybernetics). The standard error of

842 the mean (SE_{mean}) was calculated as the standard deviation divided by the square root

843 of the number of images.

Supplementary Table S1. Oligonucleotide probes used for fluorescence in situ hybridization (FISH)

Probe	Probe sequence (5'-3')	Specificity	FA (%)	Reference
EUB 338	GCTGCCTCCCGTAGGAGT	Most Bacteria	35	Daims et al., 1999
EUB 338-II	GCAGCCACCCGTAGGTGT	Planctomycetales and other Bacteria	35	Daims et al., 1999
EUB 338-III	GCTGCCACCCG AGGAGT	Verrucomicrobiales and other Bacteria	35	Daims et al., 1999
PAO462	CCGTCATCTACWCAGGGTATTAAC	Most <i>Accumulibacter</i> spp.	35	Crocetti et al., 2000
PAO651	CCC TCT GCC AAA CTC CAG	Most <i>Accumulibacter</i> spp.	35	Crocetti et al., 2000
PAO846	GTTAGCTACGGCACTAAAAGG	Most <i>Accumulibacter</i> spp.	35	Crocetti et al., 2000
Acc-I-444	CCCAAGCAATTTCTTCCCC	Most <i>Accumulibacter</i> I	35	Flowers et al., 2009
Acc-II-444	CCCGTGCAATTTCTTCCCC	Most <i>Accumulibacter</i> IIA, IIC and IID	35	Flowers et al. , 2009
ALF969	TGGTAAGGTTCTGCGCGT	Most Alphaproteobacteria	35	Crocetti et al., 2002
GAOQ431	TCCCCGCCTAAAGGGCTT	Some <i>Competibacter</i> spp.	35	Crocetti et al., 2002
GAOQ989	TTCCCCGGATGTCAAGGC	Some <i>Competibacter</i> spp.	35	Crocetti et al., 2002
GB_G2	TTCCCCAGATGTCAAGGC	Some <i>Competibacter</i> spp.	35	Kong et al., 2002
TFO_DF218	GAAGCCTTTGCCCTCAG	Some <i>Deffluvicoccus vanus</i>	35	Wong et al., 2004
TFO_DF618	GCCTCACTTGTCTAACCG	Some <i>Deffluvicoccus vanus</i>	35	Wong et al., 2004
DF988	GATACGACGCCCATGTCAAGGG	Some <i>Deffluvicoccus vanus</i> spp.	35	Meyer et al., 2006
DF1020	CCGGCCGAACCGACTCCC	Some <i>Deffluvicoccus vanus</i> spp.	35	Meyer et al., 2006

844

845 **Text S3. The detailed explanation for the PHA synthesis mechanism during**
846 **anaerobic starvation**

847 The PHA composition depends greatly on whether PAOs selectively or randomly
848 condense activated acetyl-CoA and propionyl-CoA to form PHA. Oehmen et al. (2006)
849 proposed that the stoichiometry of PAOs fed with propionate were closely correlated
850 with the model based on selective condensation of activated acetyl-CoA and
851 propionyl-CoA, while GAOs tend to randomly condense activated acetyl-CoA and
852 propionyl-CoA in PHA formation. Lemos et al. (2003) concluded that the notable
853 difference in the components of PHA in various studies is probably due to different
854 populations and/or metabolisms. Because there were more GAOs ($27 \pm 0.5\%$) in
855 nitrate-DPAOs, a better prediction was obtained by Eq. (2) (*Section 4.1.1*), which was
856 based on the random condensation pattern. Conversely, the relatively high PH₂MV
857 content means a larger amount of activated propionyl-CoA production and/or a more
858 preferentially selective binding together of activated propionyl-CoA molecules. The
859 exact underlying reason for this requires further investigation.
860

861 **Text S4. The maintenance energy calculation of poly-P, glycogen and**

862 **polysaccharides in the EPS**

863 The maintenance energy production by DPAOs was calculated from the amounts of
864 glycogen consumption and poly-P hydrolysis, based on the assumption of hydrolysis
865 of 1 mol poly-P yielding 1 mol ATP, and degradation of 1 mol-C glycogen producing
866 0.5 mol ATP (Smolders et al., 1994).

867 The content of polysaccharides in EPS was also measured using the anthrone
868 method (Frølund et al., 1996), the same as that of glycogen, which is determined by
869 total carbohydrates using glucose as the standard. 1 mol-C polysaccharides in EPS is
870 deduced to produce 0.5 mol ATP, according to the existed conclusion that degradation
871 of 1 mol-C glycogen produces 0.5 mol ATP (Smolders et al., 1994).

872

873

874 **Figure captions**

875 **Figure S1** Variations in nutrients and carbon profiles during a typical cycle in

876 SBR_{NO3-} and SBR_{NO2-}

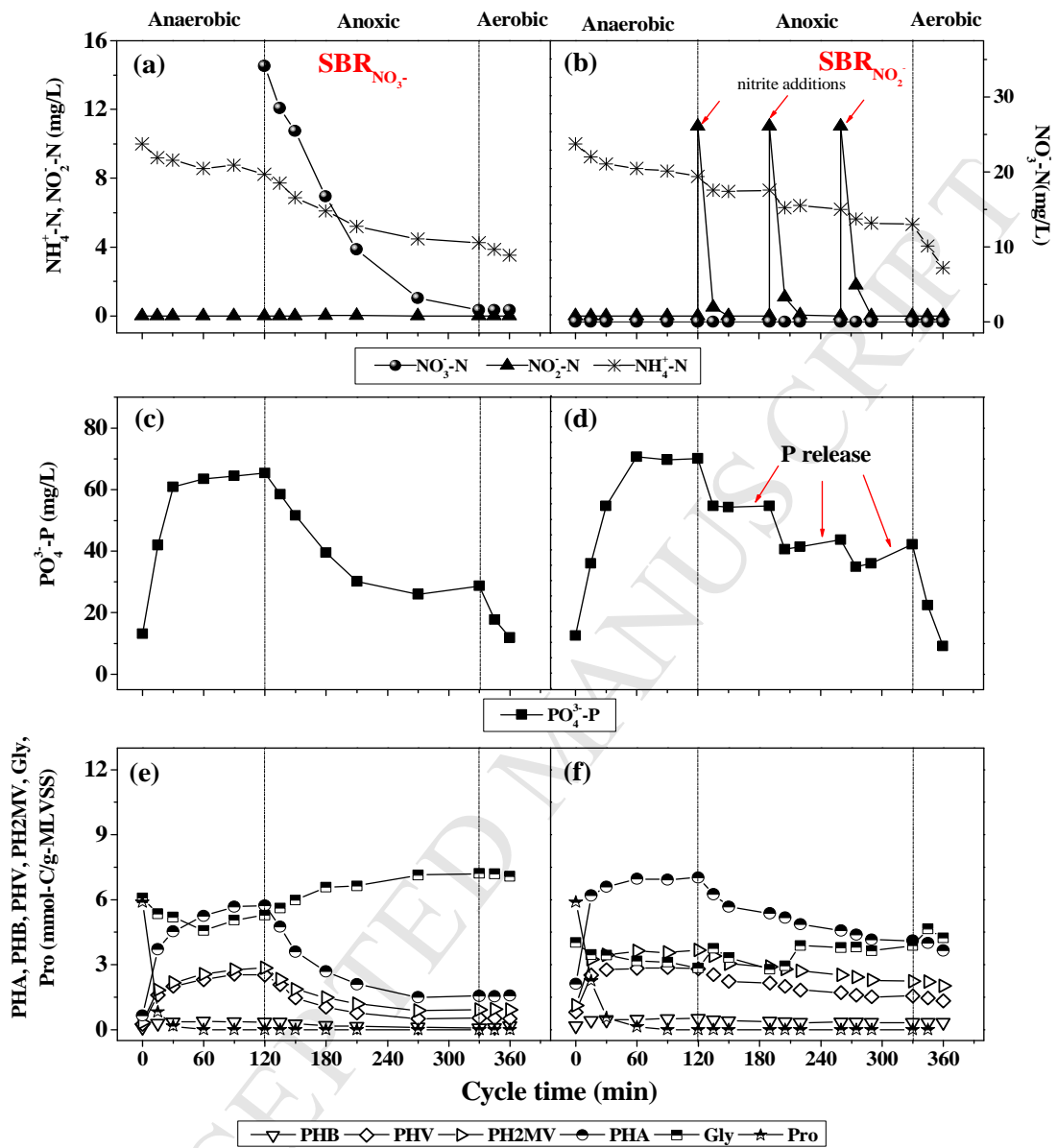
877

878

ACCEPTED MANUSCRIPT

879 Fig. S1

880



881

882

883 Fig. S1. Variations in nutrients and carbon profiles during a typical cycle in $SBR_{NO_3^-}$ and $SBR_{NO_2^-}$.

884

885

886

887

888 **References**

- 889 Amann, R.I., 1995. Fluorescently labelled, rRNA-targeted oligonucleotide probes in the study of
890 microbial ecology. *Mol. Ecol.* 4 (5), 543–554.
- 891 Crocetti, G.R., Banfield, J.F., Keller, J., Bond, P.L., Blackall, L.L., 2002. Glycogen-accumulating
892 organisms in laboratory-scale and full-scale wastewater treatment processes. *Microbiology.*
893 148 (11), 3353–3364.
- 894 Crocetti, G.R., Hugenholtz, P., Bond, P.L., Schuler, A., Keller, J., Jenkins, D., Blackall, L.L.,
895 2000. Identification of polyphosphate-accumulating organisms and design of 16S
896 rRNA-directed probes for their detection and quantitation. *Appl. Environ. Microb.* 66 (3),
897 1175–1182.
- 898 Daims, H., Brühl, A., Amann, R., Schleifer, K., Wagner, M., 1999. The Domain-specific Probe
899 EUB338 is Insufficient for the Detection of all Bacteria: Development and Evaluation of a
900 more Comprehensive Probe Set. *Syst. Appl. Microbiol.* 22 (3), 434–444.
- 901 Flowers, J.J., He, S., Yilmaz, S., Noguera, D.R., McMahon, K.D., 2009. Denitrification
902 capabilities of two biological phosphorus removal sludges dominated by different *Candidatus*
903 *Accumulibacter* clades. *Environ. Microbiol. Rep.* 1 (6), 583–588.
- 904 Frølund, B., Griebe, T., Nielsen, P.H., 1995. Enzymatic activity in the activated-sludge floc matrix.
905 *Appl. Microbiol. Biotechnol.* 43 (4), 755–761.
- 906 Frølund, B., Palmgren, R., Keiding, K., Nielsen, P.H., 1996. Extraction of extracellular polymers
907 from activated sludge using a cation exchange resin. *Water Res.* 30 (8), 1749–1758.
- 908 Lemos, P.C., Serafim, L.S., Santos, M.M., Reis, M.A., Santos, H., 2003. Metabolic pathway for
909 propionate utilization by phosphorus-accumulating organisms in activated sludge: ¹³C
910 labeling and in vivo nuclear magnetic resonance. *Appl. Environ. Microb.* 69 (1), 241–251.
- 911 Li, X. Y., Yang, S. F., 2007. Influence of loosely bound extracellular polymeric substances (EPS)
912 on the flocculation, sedimentation and dewater ability of activated sludge. *Water Res.* 41 (5),
913 1022–1030.
- 914 Kong, Y.H., Ong, S.L., Ng, W.J., Liu, W.T., 2002. Diversity and distribution of a deeply branched
915 novel proteobacterial group found in anaerobic–aerobic activated sludge processes. *Environ.*
916 *Microbiol.* 4 (11), 753–757.
- 917 Meyer, R. L., Saunders, A. M., Blackall, L. L., 2006. Putative glycogen accumulating organisms
918 belonging to Alphaproteobacteria identified through rRNA-based stable isotope probing.
919 *Microbiology.* 152 (2), 419–429.
- 920 Oehmen, A., Keller-Lehmann, B., Zeng, R.J., Yuan, Z.G., Keller, J., 2005. Optimisation of
921 poly-beta-hydroxyalkanoate analysis using gas chromatography for enhanced biological
922 phosphorus removal systems. *J. Chromatogr. A* 1070 (1), 131–136.
- 923 Oehmen, A., Zeng, R.J., Saunders, A.M., Blackall, L.L., Keller, J., Yuan, Z., 2006. Anaerobic and
924 aerobic metabolism of glycogen-accumulating organisms selected with propionate as the sole
925 carbon source. *Microbiology* 152 (9), 2767–2778.
- 926 Wong, M., Tan, F.M., Ng, W.J., Liu, W., 2004. Identification and occurrence of tetrad-forming
927 Alphaproteobacteria in anaerobic–aerobic activated sludge processes. *Microbiology* 150 (11),
928 3741–3748.

Highlights (85 characters)

- ▶ Anaerobic starvation (12d) and recovery of nitrite-DPAO was studied for the first time
- ▶ EPS polysaccharides were an additional maintenance energy source for DPAO' survival
- ▶ Maintenance energy and cell decay were lower for nitrite- than nitrate-DPAO sludge
- ▶ Nitrite-DPAO had better stringent response to the starvation than nitrate-DPAO
- ▶ Nitrite-DPAO sludge had faster starvation recovery than nitrate-DPAO sludge